# Development of a 6-DOF Robotic Test System for Studying the Biomechanics of Total Knee Replacement

by

Ephrat Most

BSE Biomedical Engineering
The University of Iowa, 1998

Submitted to the Department of Mechanical Engineering
in Partial Fulfillment of the Requirements for the Degree of
Master of Science in Mechanical Engineering
at the

MASSACHUSETTS INSTITUTE OF TECHNOLOGY

June 2000



Author.....
Department of Mechanical Engineering
May 19, 2000

Certified by.....
Guoan Li
Assistant Professor of Orthopedic Surgery/Bioengineering
Harvard Medical School
Thesis Supervisor

Certified by.....
Derek Rowell
Professor of Mechanical Engineering
Thesis Supervisor

Accepted by.....
Ain A. Sonin
Chairman, Department Committee on Graduate Students

# Development of a 6-DOF Robotic Test System for Studying the Biomechanics of Total Knee Replacement

by

Ephrat Most

Submitted to the Department of Mechanical Engineering
in partial fulfillment of the requirements for the degree of
Master of Science in Mechanical Engineering

## Abstract

A robotic-based joint testing system for studying the biomechanics of Total Knee Arthroplasty (TKA) was developed in this project. The system is composed of a 6 Degree-of-Freedom (DOF) robotic manipulator (Kawasaki UZ150®) and a 6-DOF universal force-moment sensor (JR3®). This testing system offers the ability to operate with force and displacement controls and is capable of characterizing the *in-vitro* kinematics and the *in-situ* forces in tissue components of the human knee. In a knee test, the femur is rigidly fixed on a pedestal while the tibia is rigidly mounted to the robot arm through the load cell. This robotic system determines the kinematics response of the knee under various external-loading conditions. The kinematics data can then be reproduced on the knee specimen. Upon simulation of knee motion, forces and displacements are evaluated from the load cell and the robot, respectively. Various TKA designs can be tested on the same specimen where the native knee is used as the reference for the evaluation of the biomechanical response of the TKA. The system could be further modified to determine optimal designs of various artificial joint replacements, using normal joint biomechanics as an objective function.

Thesis Supervisor: Guoan Li
Title: Assistant Professor of Orthopedic Surgery/Bioengineering, Harvard Medical School

Thesis Supervisor: Derek Rowell
Title: Professor of Mechanical Engineering

To my parents:

Nathaniel (ז״ל) and Ruth Most

Anyone who has never made a mistake has never tried anything new.
- Albert Einstein

## Acknowledgments

These past two years have been more than astonishing. I can clearly remember my first day at MIT. I was overwhelmed! Everything had a number and everyone referred to things as a number. It took me at least an hour to find building 1 (Mechanical Engineering office). At that time, it seemed reasonable to assume that building 1 is right next door to building 2, but it is not. I want to thank the people that helped me in my early days at MIT to the present. I want to single out a few special people.

First and foremost, I want to thank my advisors: Drs. Guoan Li, Derek Rowell, Harry Rubash, and James Herndon. It has been an honor and a privilege to work with such knowledgeable and experienced faculty. I especially want to thank Dr. Li who spent hours and hours patiently teaching me step-by-step the secrets of mechanical engineering and biomechanics. Dr. Li, you have been more than a mentor to me. Your knowledge, motivation, encouragement, and advice will be a role model in my career. I admire your patience and guidance even when I fell short of your expectations. I express my gratitude to Dr. Rowell for guiding me through my MIT experience, offering insight in system development, providing me with thesis guidance, and allowing me to simply stop by his office to tell him what is on my mind. Drs. Rubash and Herndon, I want to thank you both for allowing me to participate in this research. This is a very exciting field and it is my honor to work with you. Dr. Rubash, I cannot thank you enough for always finding time for me and my husband in your extremely busy schedule.

This work could not be done without the assistance of many other people. Leslie Regan, Joan Kravit, Bridget Riley, and Lori Humphrey; I could not have done it without

you! Thank you for all your help and guidance throughout these past two years. You have a special place in my heart (and in my teeth from all the candy that you provided me).

I thank the members of the Orthopedic Biomechanics Laboratory (OBL), past and present, who have been there academically as well as socially. I thank each and every one of you for helping me when needed, for keeping me on my toes when I did not clean the tools, and for simply being there as friends. I am proud to be a member of the OBL! I deeply thank my lab partner, Lou DeFrate, for his energetic spirit and keen insights.

I would like to thank Maria Apreleva, Jennifer Copper, and Melissa Pierre who had taken time to review this work and offer comments to improve its presentation.

None of the TKA surgeries would have been possible without the cooperation and talent of Erik Ottorberg.

Part of my research involved testing of human cadavers. I want to thank the donors and their families for believing in improving the human conditions. Your generosity has been a tremendous contribution to knee biomechanics research.

I wish to thank a pioneer in the field of Musculoskeletal Biomechanics research, Dr. Savio L-Y. Woo. Dr. Woo gave me the opportunity as an undergraduate student to take part in the MSRC summer internship research program. This was a real turning point in my academic career.

I express my thanks to two more people who had a tremendous influence on my educational career: Drs. Vijay Goel and Lars Gilbertson who believed in me from the beginning.

Last but not least, I want to thank my family for all their support and sacrifices throughout the years. From the bottom of my heart I thank my mother, Ruth Most, for giving me the best I can get, often, more than I deserved. To my sisters, Liora (Lulu) and Ayala (Ayal) for helping mom when I was away and keeping me up-to-date with all the gossip over in Israel. To my husband, Sheldon: there are not enough words and space to express my thanks to you. You have been the light of my life. I could not have done it without you!

I remember with love, the first engineer in my life, my father Nathaniel Most (ז"ל). I walk in your shoes.

This work was funded by the National Science Foundation (NSF). TKA components were generously provided by Zimmer.

Ephrat (Ephi) Most.

# Contents

# List of Figures

# List of Tables

# Chapter 1

# INTRODUCTION

## 1.1 Motivations and Objectives

Human knee joints are subjected to a wide range of forces during daily activities. These forces can be several times body weight for activities such as climbing stairs or rising up from a chair and can be as high as 10 to 20 times body weight for activities such as jumping or running. It is remarkable that the human joint can undergo millions of cycles under such high forces. However, there are many observations of human joint degeneration that eventually lead to surgical intervention. Joint degeneration is poorly understood, but there is no doubt that these high forces contribute to such a process [1-3].

Common symptoms of joint degeneration are reduced joint flexibility, development of bony spurs, joint pain, and swelling of the joint [4]. Osteoarthritis (OA) is one of the major degenerative joint diseases that develop in joints that are injured by repeated overuse in the performance of a particular activity or from carrying excess bodyweight. OA is frequently associated with aging due to general wear and tear in the joint. People with severe OA have problems performing even the simplest daily activities such as walking or getting up of a chair. An estimated 16 million Americans are

afflicted with OA. About 65% of the people with OA are over the age of 65. More men than women under the age of 45 have OA, but twice as many women as men over the age of 65 experience these conditions.

Total knee arthroplasty (TKA) has been a popular surgical procedure to treat people with severe degenerative joint disorder such as OA. This surgery is also performed to replace a badly fractured knee and when previous joint replacements have failed. The femoral component of a TKA is usually made of an alloy containing chromium, cobalt and molybdenum that are nearly inert in the body. The tibial component is often made of titanium that is lighter, stronger and leaves more space for the plastic bearing surfaces. The plastic is ultra high molecular weight polyethylene (UHMWPE), chemically similar to ordinary polythene but immensely hard and very smooth (Figure 1.1) [84].

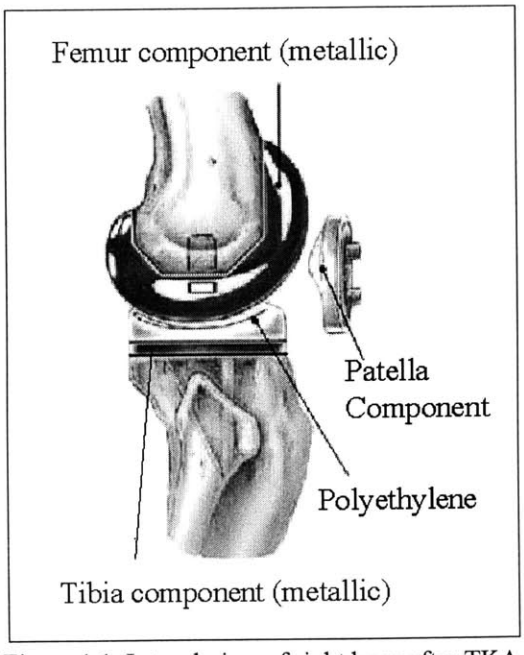


Figure 1.1: Lateral view of right knee after TKA.

In 1994, there were 230,342 TKA surgeries performed in the United States; 211,872 primary TKAs and 18,470 revisions [5]. Further, in 1997, the number of inpatient procedures for arthroplasty and knee replacement increased to 338,000 [National Center for Health Statistics, National Hospital Discharge Survey, 1997]. TKA implants do not last indefinitely in the joint. The main mechanisms for TKA failure are loosening of the prosthesis from the bone, joint infection, polyethylene wear, component instability, poor range of motion, bone fracture, and patella complications. The joint may need to be changed but the second operation, which is more difficult than the first, may not be as successful and the knee may need to be stiffened [6-7].

Even though TKA is a popular procedure, the exact mechanisms that play a role in its success or failure are unknown. It is unclear about the exact role of the ligaments, patella, patella tendon, and muscle loading on both the kinematics (motion) as well as the kinetics (forces) of the knee after TKA. Limited information is available regarding both magnitude and location of the contact stresses within the artificial knee joint.

One of the most controversial issues regarding TKA is the role of the posterior cruciate ligament (PCL). Two schools of thoughts regarding the PCL contribution to TKA outcome can be found in the literature. Some researchers found that the PCL plays an important role in the restoration of normal knee function post TKA. Others reported that the PCL might contribute to complications after TKA. PCL retention has been advocated for its effect on keeping the femoral component rolling motion on the tibial plateau, and reducing tibial shear forces [8-12]. Others demonstrated that the PCL does not always cause posterior roll back of the femur in squatting, which might accelerate polyethylene liner wear on TKA [13]. Further, inadequate PCL tension may cause

abnormal kinematics following TKA. Inconsistent results regarding the surface strain of the PCL have been reported in the literature [14, 15]. In spite of extensive research the biomechanical role of the PCL in TKA remains unclear. Additional information (e.g. the constraint forces of the PCL) is needed for a more objective rather than subjective TKA. A method / system for quantitatively evaluating the mechanisms involved with TKA is desired.

The primary objective of this work is to develop a non-contact experimental system for the quantification of PCL tension and tibio-femoral joint forces of the knee under physiological loads. The system is composed of a 6 degree-of-freedom (DOF) robotic manipulator and a 6 DOF load cell. This system determines knee joint motion under simulated muscle loads and measures ligament forces using the principle of superposition instead of attaching a sensor onto the target ligament. Using this system, it is possible to study the role of the PCL on TKA and to quantify the contact forces at the medial and lateral sides of the knee pre- and post- operatively for a variety of knee joint replacement implants. This information is important for joint stability and for the analysis of polyethylene wear. Key advantages of this system are repeatability, the non-contact measurements, and the capability to limit intra-specimen variation by performing multiple tests on the same knee specimen (intact knee, knee after various surgical modification, etc.).

## 1.2 Organization

This dissertation reports the development of a 6-DOF robotic system for studying the biomechanics of total knee joint replacement. The central focus is on the development of the system, its uniqueness and its future applications.

The text is organized sequentially. Chapter 2 contains a review of the anatomy and the biomechanics of the human knee. In addition, a literature review of relevant work both on the native knee as well as the TKA knee is presented. Chapter 3 reports a description for each of the components that make up the robotic testing system. The robotic system has both position and force control capabilities. In Chapter 4, the reader can find a description of how the system works. The final chapter presents the overall results of this project as well as suggestions for future directions of this project.

# Chapter 2

# ANATOMY AND BIOMECHANICS OF THE HUMAN KNEE

In order to provide the fundamental background of this project, this chapter presents basic information in two areas. First, a detailed description of human knee anatomy is presented. Second, a literature review on knee joint biomechanics is presented.

## 2.1 Knee Anatomy

The knee is perhaps one of the most complicated joint in the human body. Mechanically, the two main functions of the knee are stability and mobility. The knee transmits loads, participates in motion, aids in conservation of momentum, and provides a force couple for activities involving the leg. Its articulating surfaces are frequently exposed to contact stresses and strains. The knee is a three-component structure (femur, tibia, and patella – Figure 2.1) that not only sustains high forces but also is located between the body's two largest lever arms. Therefore, it is susceptible to injuries and chronic diseases such as ligament rupture, meniscal tear, dislocations, arthritis, etc. Understanding of knee joint kinematics and tissue forces in response to external loads is crucial in the diagnosis of

joint disorders resulting from either an injury or a disease. Moreover, comprehensive knowledge of knee function plays an important role in the design of prosthetic devices as well as post-operative rehabilitation. In the following sections, the main components of the knee joint are described.

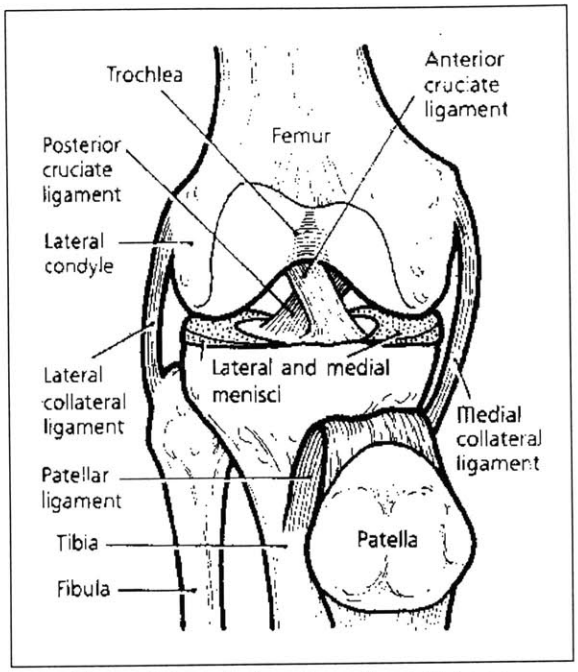


Figure 2.1: Anterior view of a right knee.

### 2.1.1 The Ligaments

Ligaments, which connect bone to bone, are soft tissues composed of closely packed, parallel collagen fiber bundles oriented to provide for the motion and the stability of the musculoskeletal system. Two ligament groups are presented in the knee (Figure 2.1). The collateral ligaments are parallel to each other and are attached to the medial and lateral sides of the knee. The cruciate ligaments are interwoven and are found in the center of the knee joint [16-19].

The cruciate ligaments account for a considerable amount of overall knee stability. The Anterior Cruciate Ligament (ACL) is an intracapsular and extrasynovial structure

approximately 11 mm wide and 31 to 38 mm long [20]. The ACL proceeds superiorly and posteriorly from its anterior medial tibial attachment to the medial aspect of the lateral femoral condyle. The ACL is a primary constraint of the anterior tibia translation. The Posterior Cruciate Ligament (PCL) is named for its posterior tibial insertion. The PCL crosses from the back of the tibia in an upward, forward, and medial direction and attaches to the anterior portion of the lateral surface of the medial condyle of the femur. The PCL acts as a drag during the gliding phase of motion and resists posterior translation of the tibia. In general, the PCL prevents hyperextension of the knee and prevents the femur from sliding forward during weight bearing. The ACL and the PCL cross each other (at $90^{o}$ of flexion).

The Lateral Collateral Ligament (LCL) and the Medial Collateral Ligament (MCL) are present in the knee as vertical ligaments. The MCL is generally divided into superficial and deep portions separated by a small bursa and a thin layer of fat, which helps to reduce friction during knee flexion. The superficial component of the tibial collateral ligament is a narrow structure of 8 to 10 cm long. It arises from the medial femoral condyle and extends inferiorly to insert on the tibia about 5 cm below the joint line [18, 19]. The MCL provides primary valgus stability to the knee joint. The LCL provides lateral stability to the knee against varus and external rotation forces [21].

The shape, length, orientation, and properties of these ligaments affect the kinematics of the knee. Moreover, for better knee joint function, the geometry of the ligaments and the geometry of the articulating surfaces are interdependent.

### 2.1.2 The Muscles

The knee is motored and stabilized by muscles that cross the joint from the origin above the hip joint, from the entire femoral shaft, and from origin above the knee of lower leg muscles. The knee muscles can be classified into four major groups: knee extensors (anterior), flexors (posterior), adductors (medial), and abductors (lateral) [22].

The major muscle of the extensor group is the quadriceps, or front thigh, (rectus femoris, vastus medialis including the vastus medialis obliquus vastus intermedius, and vastus lateralis) which insert into the patella and the extensor retinaculum (Figure 2.2). These muscles act together to extend (straighten) the knee and to control the side-to-side movement of the patella. The flexor group can be divided into the medial and lateral groups. The hamstrings are composed of the biceps femoris muscle on the lateral aspect and the semimembranosus and semitendinosus muscles on the medial aspect [4].

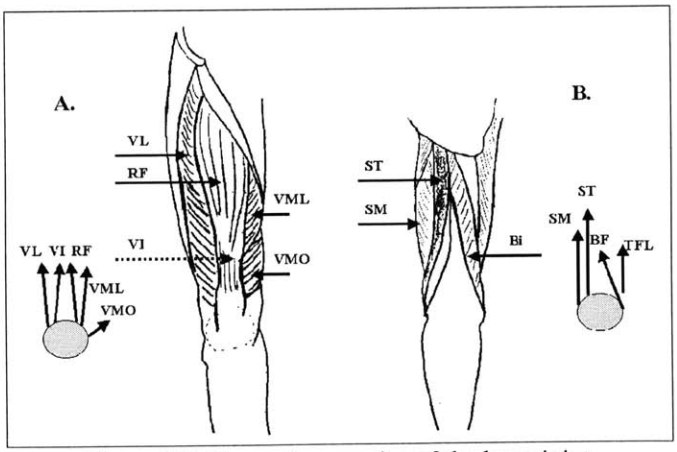


Figure 2.2: The major muscles of the knee joint.

A. Anterior view of major muscles of the knee: Quadriceps group (VL, vastus lateralis; RF, rectus femoris; VM/ VML, vastus medialis; VI, vastus intermedius; VMO, vastus medialis oblique fibers).

B. Posterior view of the major muscles of the knee: Posterior thigh muscles (ST, semitendinosus; SM, semimembranosus; Bi; biceps; TFL, tensor facia lata).

### 2.1.3 The Patella

The patella is held in place by the quadriceps tendon superiorly and the patellar ligament (also known as patellar tendon) inferiorly, as it glides through the trochlea of the femur. The underside of the patella is divided into the medial, lateral, and odd facets, each of which is covered by articular cartilage that helps with shock absorption, smooth articulation, and load distribution (Figure 2.3).

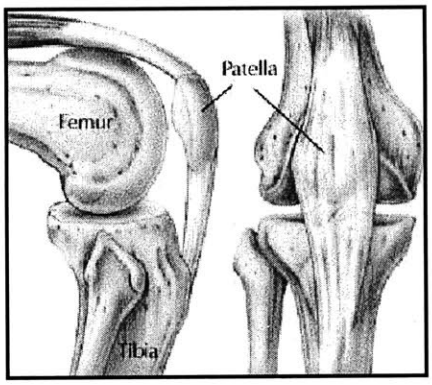


Figure 2.3: Lateral and anterior view of patella and patella tendon.

The patella serves two important biomechanical functions in the knee. First, it increases the efficiency of the quadriceps muscle by increasing its lever arm. This provides a mechanical advantage by lengthening the extension moment arm throughout the entire range of knee joint motion, but in doing so, it is subjected to considerable retropatellar compression force. Second, it allows a wider distribution of compressive stress on the femur by increasing the contact area between the patella tendon and the femur [85].

Cartilage on the undersurface of the patella is the thickest of any found in the body. This thick joint cartilage acts as a cushion, absorbing shock in the greatest weightbearing joint in the body during the process of deceleration.

### 2.1.4 The Menisci

The menisci (Figure 2.4) are two fibrocartilagenous, semilunar structures with a wedge-shaped cross-section that lie between the opposing articulating surfaces (femur and tibia).

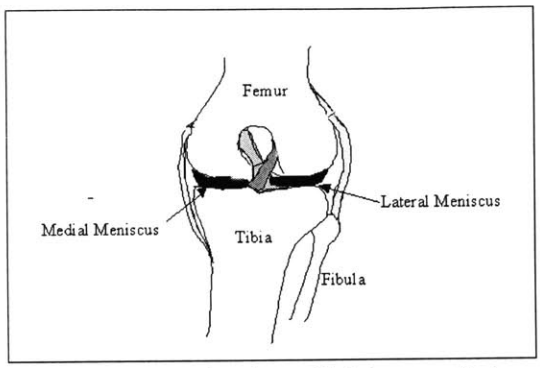


Figure 2.4: Anterior view of left knee outlining the medial and lateral menisci.

The menisci's functions are [23]:

I. To serve as shock absorption to protect the articular surfaces of the bones,

II. To eliminate most of the direct tibial-femoral contact while increasing the surface contact of the joint, thus reducing contact stress,

III. To increase the elasticity of the joint,

IV. To assist in lubrication, and

V. To provide stability and increased range of flexion.

When a load is transmitted between the femur and the tibia, the vertical component tries to squeeze the meniscus out from between the articular surfaces. Hoop tension stiffness and stress act against that squeeze, to pull the meniscal wedge in between the opposing joint surfaces to maintain close contact and evenly distributed pressure in the wedge (Figure 2.5). This tends to float the femoral condyles above the tibial condyles. During this process, the high compliance in the flexure and shear allows the meniscus to deform

and adapt readily even to rapidly changing alignments of the articular incongruities. That unit loading over the whole meniscal surface in contact with cartilage tends to remain uniform. In the case that the menisci were to be removed, this load distribution effect will be altered, causing pain, bone wear and an increase in pressure on other joints, such as the hip, due to uneven load distribution on the knee joint. [4]. These effects may eventually result in joint degeneration.

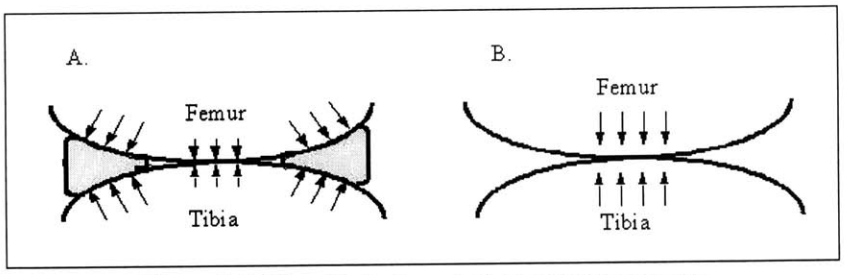


Figure 2.5: The effect of menisci on contact stresses:
A. With menisci, B. Without the menisci.

## 2.2 Current Status of Knee Joint Biomechanics

Understanding the mechanism behind the load transmission in the knee joint in response to external loads plays an important role in the clinical world. It is not surprising that knee joint behavior has been studied extensively, both experimentally and computational, in the last two decades [24-29]. This brief review outlines the current status of knee biomechanics research.

### 2.2.1 Biomechanics of the Human Knee Joint

The human knee joint has been extensively studied. In many cases, knee joint motion was measured by rotary transducers [30], linearly variable differential transducers (LVDT), or rotational-variable differential transducers (RVDT) [31-33]. The motion of the tibia relative to the femur has also been measured using stainless steel pins that were

embedded into the bone to minimize skin motion [34-39]. Lewis et al. [34] developed an experimental system to quantify *in vitro* knee joint biomechanics. The system included an Instrumental Spatial Linkage (ISL) system for measuring 3D joint motion, buckle transducers for measuring ligament forces, and a pneumatic load apparatus for the application of external load. The ISL was composed of six revolute joints connecting two end links and five intermediate links. The motion of these joints was measured by potentiometers. Both femur and tibia were clamped onto the load apparatus but only the tibia was allowed to move (i.e. the femur was rigidly fixed).

Knee motion measured via geometrical properties is another way to study knee kinematics. Kurasawa et al [40] measured 3D knee motion by using the center of the posterior femoral condyles as a reference point. They analyzed sections of the distal femur by a computer and compared that to direct measurements to show that the femoral condyles can be approximated as spherical surfaces. They determined that from fully extended knee to 120 degrees of flexion the medial femoral condyle moved less than the lateral femoral condyle. Further, they observed an axial rotation of 20 degrees.

Light emitting diodes (LED) have been successfully applied in gait studies [35, 41]. Direct measurement of skeletal motion requires an invasive procedure to place pins on the bone. In many cases, external markers are used for similar analysis. Reinschmidt et al. [35] investigated the effect of skin movement on the analysis of knee joint motion. Skin markers were attached to three subjects. To compare the measurements obtained using the skin markers, bone pins were inserted as well. 3D kinematics of running trials were recorded using high-speed cine cameras (200HZ) and compared. They found that

the average errors relative to the range of motion during running were 21% for flexion/extension, 63% for internal/external rotation, and 70% for abduction/adduction.

A number of authors have studied passive knee joint motion, laxity, and stability. Tools for control motions and external load application included instrumented handlebar [42, 43], instrumented fixtures in MTS® or Instron® testing machines [44-47]. Other investigators have used triaxial goniometer [43,48], photographic instruments [49], and roentgen-sterephotogrammetry (SPG) [24,50-56] to measure knee joint motion. Huiskes et al. [57] used analytical, closed-range sterophotogrammetry to determine the 3D geometry of the articular joint surfaces *in-vitro*. They projected a visible grid onto the articular surfaces. Glass rods with tantalum markers, firmly fixed to the bone, were used to inter-relate the articular surface geometry with the roentgenstereo-photogrammetry motion data. Blankevoort et al. [52] measured the *in-vitro* passive range of motion characteristics of the human knee joint under external loads using a 6 DOF motion rig. An accurate roentgen SPG system was applied for the measurement for geometric information. Human knees were used such that the tibia was free to move in 5 DOF relative to the fixed femur. Loading of the knee was done by applying weights to the part of the apparatus that was associated with the respective motion. Tantalum markers were placed on both bones to monitor the relative motion.

Many 6 Degree-of-Freedom (DOF) testing systems have been used for the measurement of knee joint kinematics under both *in-vivo* and *in-vitro* conditions [32, 33, 39, 52, 58-61]. Rudy et al [61-64] developed a robotics-based joint testing system that offers the ability to control both the paths of motion as well as the acting forces. The system is composed of a 6 DOF robotic articulated manipulator and a universal force-

moment sensor (UFS). The testing of the knee specimen is done with the femur rigidly fixed to the robot base while the tibia is rigidly mounted to the robotic arm through the UFS. The system provides not only the measurement of structural properties, but also the ability to store and repeat the 3D motion paths under different loading conditions. In response to external loads, the robot can learn the complex motion of the knee specimen. The system can then reproduce these motions in subsequent tests.

### 2.2.2 Biomechanics of Total Joint Replacement

Knee replacements, commonly used today, differ from each other in material, fixation design, and more fundamentally, in their articular surface design [40, 65]. This wide range of available designs reflects different interpretations of the complex geometry of the natural joint surfaces. Desirable characteristics in knee prosthesis include durability, natural feeling, and interchangeability between sizes so that the femoral and tibial components can be fitted independently to their respective bones [6]. Three major TKA designs exist on the market:

I. PCL retention (PCR), where the PCL is saved (Figure 2.6),

II. PCL sacrificing (PCSac), where the PCL is resected but no substitution is added, and

III. PCL substitution (PCSub), where the PCL is resected but the implant design compensates for the absence of PCL (Figure 2.7).

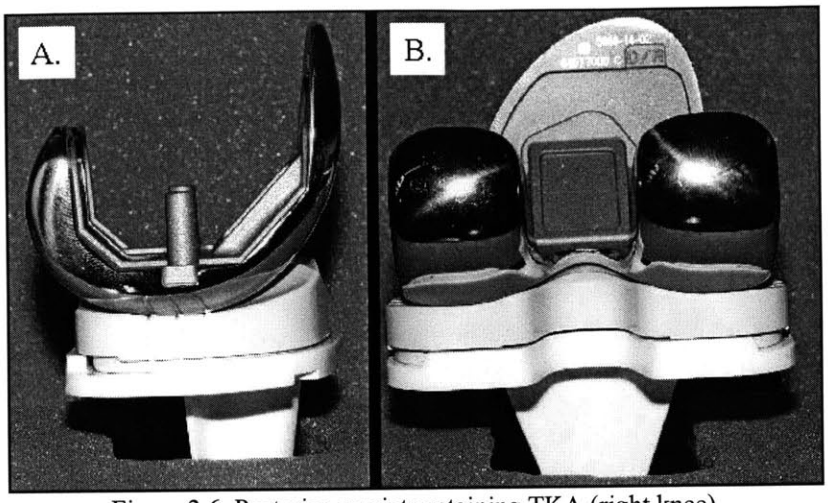


Figure 2.6: Posterior cruciate retaining TKA (right knee).
A. Lateral view, B. Posterior view.

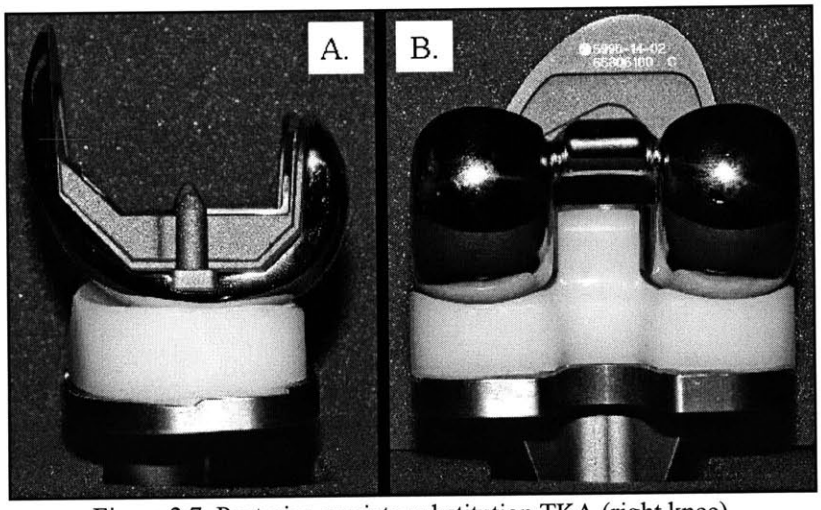


Figure 2.7: Posterior cruciate substitution TKA (right knee).
A. Medial view, B. Posterior view.

The role of PCL on knee joint function after TKA has been one of the most controversial issues in total knee replacement area. It has been argued that PCL retention in TKA can enhance joint stability, improve passive range of motion by allowing femoral roll back, increase the efficacy of the knee musculature, and reduce stresses at the cement-bone-implant interfaces [8, 66, 67]. Singerman [11] measured the surface strain of the PCL as a function of knee flexion angle and found that decreased posterior tibial slope increases strain in the PCL following TKA. Using a combined buckle transducer

technique and computer modeling, Lew and Lewis [9] reported that PCL forces with a low conformity design were similar to those in the normal knee, but were substantially higher between 60° to 90° of flexion for a high-conformity design. Follow-up studies of patients post TKA showed that partial release of the PCL is beneficial for patients with tight PCL at the time of knee arthroplasty. This partial release procedure improved maximum flexion angle and maintained anterior-posterior stability [12, 68]. It was suggested by Freeman and Railton [69] that PCL may contribute to posterior stability in a flexed knee if its tension can be accurately restored. However, normal tension of the PCL is often difficult to obtain [6]. Researchers [70, 71] analyzed the joint kinematics of TKA with PCL retention and found that physiological rollback of the femur was not demonstrated for patients after a PCL retaining TKA. Dennis et al [13] observed abnormal femoral translation during deep knee bends of patients after TKA. Further, they demonstrated that the TKA with PCL retention has a similar passive range-of-motion (ROM) to TKA with PCL substitution, but a decreased ROM during squatting compared with the PCL substituting TKA. Long term patient follow-up studies revealed no differences between knee scores or long term survival rates in patients after TKA with PCL retention and TKA with PCL substitution [65, 72, 73]. Laskin [74] reported that TKA with PCL retention in rheumatoid arthritis increased posterior instability and recurvatum deformity, resulting in an increased revision rate. Recently, there are reports showing that the preservation of the PCL in TKA may not improve knee joint proprioception and subsequently may not improve TKA functional performance [41, 75].

# Chapter 3

# ROBOTIC TESTING SYSTEM FOR TKA BIOMECHANICS

The desired purpose of a TKA is to restore normal joint function, which includes both kinematics and kinetic restorations. Hence, the TKA should restore the knee joint motion in 6-DOF as well as, joint pressure, ligaments tension, and patella contact mechanics. It is a challenge to quantify the biomechanical responses of the intact knee and the knee after TKA using the same knee specimen.

It is therefore the objective of this project to develop a non-contact, 6-DOF experimental system for measuring knee kinematics, tibio-femoral joint forces and ligaments forces under simulated external loading conditions. The test system is composed of a 6 degree-of-freedom (DOF) robotic manipulator (Kawasaki UZ150®, Kawasaki Heavy Industry, Japan) and a 6 DOF load cell (JR3 DSP-based force sensor receiver, JR3 Inc., Woodland, CA). A control algorithm that uses global convergence method [77] that considers the coupling effects of the different DOF of the knee was developed in this project. This algorithm links the robot and the load cell so that both displacement and force controls are available.

# 3.1 Displacement Control Device: Robot Manipulator

## 3.1.1 General Description[1]

The robotic system is composed of two main components: the robotic arm manipulator and the C controller (Figure 3.1). The Kawasaki UZ150® manipulator consists of rigid links which are connected with six joints that allow relative motion of the neighboring links. The manipulator is equipped with six stepper motors that can directly execute a desired trajectory (position control capability). A movement of the manipulator to follow a desired route is achieved by a position control system that uses feedback from joint sensors to keep the manipulator on course. The C controller offers a large, multi-functional color liquid crystal display (LCD) that combines the functions of a conventional teach pendant with several specialized displays on an 8-inch touch panel. Easy block-step programming and high-end AS language programming are both available. This AS language allows a wide range of robot control commands, numerical calculations, conditional jump step divergence, interrupt I/O and program creation on PC. The controller's multitasking capability allows parallel programs to run simultaneously while the robot is moving, and simple sequences do not require the use of a sequencer.

---

[1] Kawasaki robot controller, A/AD series manual, 4th edition.

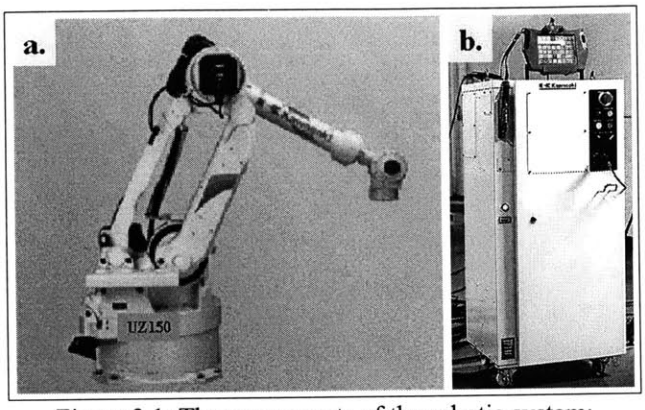


Figure 3.1: The components of the robotic system:
a. Kawasaki UZ150 manipulator; b. C-Controller.

Table 3.1 summarizes some of important specification of the UZ150 model.

Table 3.1: UZ150 selected specification.

| Axes | Payload | Repeatability |
|---|---|---|
| 6 | 150 Kg | ±0.3 mm |

The repeatability value reported here is for full load, extended arm, and high-speed (1000mm/sec) operation. For a more confined space and slower speed as used in the knee joint experiment, this value is reduced dramatically.

### 3.1.2 Communication with Personal Computer (PC)

The robotic system can be controlled either by the C-controller (AS language) or by a host computer via a serial port. In this project, a personal computer (Dell Dimension 3DX) was used in the control procedures. A serial (RS232) interface was constructed between the C controller and the PC to allow information on the robot location to be transferred between the two systems. Through a specified protocol, ASCII characters were sent and received on the serial interface line. A basic handshaking protocol was used in this project (Figure 3.2).

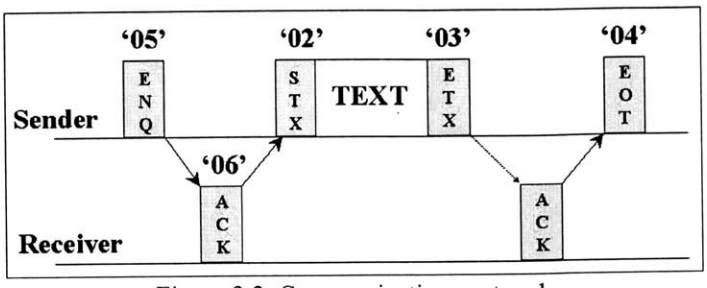


Figure 3.2: Communication protocol.
(ENQ, query; ACK, acknowledgment; STX, start text; ETX, end of text; EOT, end of transmission)

Both the controller and the PC had to be programmed to communicate with each other following the above protocol. A Visual Basic (VB, Microsoft® Visual Basic 6.0) code was developed for the PC and AS code was written for the controller. In this project, the current position of the robot is crucial at all times. This is done by the robot sending its location using the AS command *SEND 2: $out, err* and the PC reading the ASCII dada using VB code *C = MSComm1.Input*. The robot command for receiving information from the PC is *RECEIVE 2: $inp, err*, while the VB code for sending information to the robot is *MSComm1.Output = a*. All communication programs developed in this project are listed in Appendix B.

## 3.2 Force Control Device: JR3 Universal Force/Moment Sensor

### 3.2.1 General Description[2]

The addition of the 6-DOF JR3® Digital-Signal-Processing (DSP, analog Devices ADSP-2105) load cell onto the end effector of the robotic manipulator provides the system with

---

[2] JR3, Inc, software and installation manual, November 1994.

the ability to control forces applied to the knee joint (force control capability). The JR3 system provides the user with decoupled and digitally filtered force and moment data at 8 kHz per channel. The system uses a dual ported Random-Access-Memory (RAM) that the user and the JR3 DSP can both read and write to. Forces and moments are written by the JR3 DSP into this RAM. The user can then read the data from the RAM. The dual-ported address space consists of 16K 2-byte words. The first 8K of this space are used as RAM while the second half consists of status registers and other features. The DSP performs several functions such as offset removal, saturation removal, digital low-pass filtering, peak detection, force and moment vector calculations, threshold monitoring, rate calculations, and coordinate system translation and rotation. The raw data from the sensor is decoupled and passed through a series of low-pass-filters (LPF). There are eight filters; the first filter has a cutoff frequency of 500Hz and each succeeding filter has a cutoff frequency of 1/4 of the preceding filter (i.e. 500Hz, 125 Hz, 31.5Hz, 7.81Hz, etc). The delay through the filters can be approximated as the inverse of the cutoff frequency. For example, the delay through the third filter (31.5 Hz) would be $1/31.5 \approx 31.7$msec.

The data structure declarations of the JR3 system are formatted in 'C' style code. The following code outlines several important definitions used in the AS code. The code defines a signed 16-bit integer value, uses an array to include force and moment data, as well as read and write from a given address:

```
int fx                          /* signed 16-bit value for storing the x component of the force */
unsinged data_array[6]          /* unsigned 16-bit array to include 3 forces and 3 moments */
readData (0xf005)               /* read the version number of the DSP software */
writeData (0x00e7, 0x0800)      /* write the value 0x800 to the 0x00e7 location */
```

JR3 DSP data locations are summarized in Appendix C.

### 3.2.2 JR3 DSP Based Force Sensor Receiver Card

The receiver card plugs into a 16-bit connector on the ISA bus. The receiver operates typically on 5V and 650mA, obtained directly from the ISA card.

The DSP receiver board uses two 16-bit wide registers. The address register is at I/O addresses zero and one relative to the base address. In this project the base address was set to 0x314. It can be concluded that the first 16-bit port at 0x314 represents the address port while the second 16-bit port, i.e. 0x316, represents the data port. The card address can be changed to fit other addresses by selecting the right switch combination. Figure 3.3 demonstrates the switch position for 0x314 address.

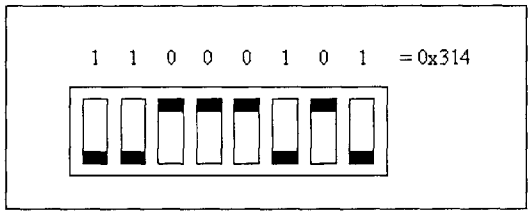


Figure 3.3: Address selection for the ISA bus receiver.

### 3.2.3 System Set-up: Force and Moment Measurements

As mentioned before, unfiltered data, as well as filtered data, can be collected from the sensor. Although all filters meet our criteria, in this project, data subsequent to the third filter (low pass filter of 31.5 Hz) has been used (data address &HA8). The data collection program is based on a previous program written by Commotion Technology (Commotion Technology, Inc. World Trade Center, Suite 250-L, San Francisco, CA 94111). The general loop for reading forces and moments is listed below:

*JR3read(boardNum, C_FORCE + i, force)*

Where:

*bourdNum* is the board number (0x314),

*C_FORCE* is the address for the force / moment data (0xa8),

*i* is the index for consecutive loop operations for three forces and three moments, and

*force* is the returned value from the sensor.

Different JR3 sensors make use of different measurement units. The JR3 2000N load cell, used in this project, makes use of SI units (N, Nm*10 for forces and moments, respectively). Note the moment units as being multiplied by ten. This is done for a more accurate reading of the lower end of the moment scale.

The capacity of JR3 load cell used in this project is shown in Table 3.2 below.

Table 3.2: JR3 sensor specific information.

| Model | Dimension | Loads[3] |
|---|---|---|
| 160M50S | 160mm diameter<br>50mm thickness | 2000N<br>250Nm |

### 3.2.4 Zeroing the Load Cell

As in every engineering system, a reference point (level) must be determined. Therefore, all values of the load cell had to be zeroed at the beginning of the experiment such that all other measured values are with respect to this zero. The following code was written in VB to zero the force and moment values of the load cell. Note that this procedure is only done once and at the beginning of each experiment.

```
Private Function zeroJR3() As Boolean

    Dim i As Integer, value As Integer, error As Long, offset As Integer
    '6 components: 3 forces 0,1,2 and 3 moments 3,4,5
    For i = 0 To 5
        ' Read current offset
        error = JR3read(0x314, 0x88 + i, offset)
```

[3] The sensor load rating is the full scale rating for the X or Y axis. The Z axis full scale rating is twice the sensor rating.

```
            If error <> 0 Then
                    Err.Raise vbObjectError + error
            End I
            ' Read current force
            error = JR3read(0x314, 0xa8+ i, value)
            ' Update current offset
            error = JR3write(0x314, 0x88 + i, offset + value)
        Next I
        ZeroJR3=True
End Function
```

This general procedure involves reading:

I. The offset for each of the variables (three force components and 3 moment components) from the DSP 0x88 location

II. The force and moment components (six total) from the DSP 0xa8 location. This location displays the data from filter #3.

Once these two quantities are read, a correction is made to the corresponding offset addresses.

### 3.2.5 Load Cell Calibration

The stability of the load cell over time is critical in this project since a typical testing session lasts about 15 hours. Further, the accuracy of the load cell had to be determined to ensure its suitability for the project (see section 4.2). Therefore, calibration of the load cell was performed in two ways. First, the response of the load cell readings over time was recorded to ensure that drifting, due to internal electronic devices, is minimal. Second, the response of the load cell to external loads was obtained by using standard weights. Figures 3.4, 3.5, and 3.6 display the results for the calibration process.

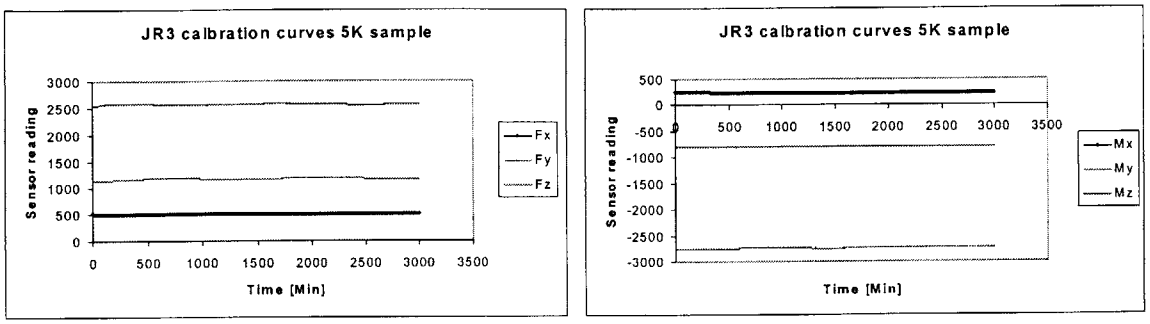


Figure 3.4: Forces and moments drifting behavior of the JR3[4] during 50 hours of operation.

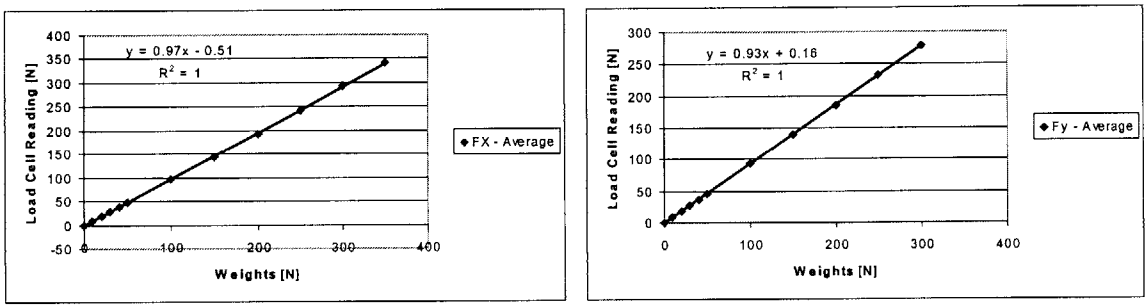


Figure 3.5: Force calibration in the x and y directions.

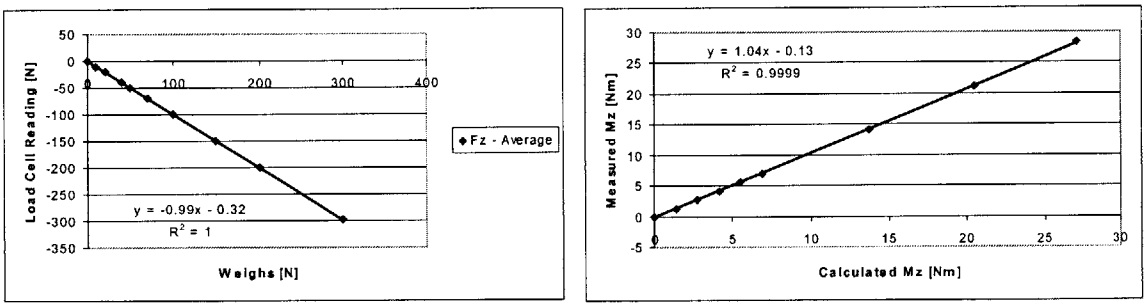


Figure 3.6: Force (z direction) and moment (around z) calibration.

Similar results were obtained for the moment around X and Y axes. The above results show that the load cell meets the calibration standards set for this project.

[4] Collaborated with Wayne Johnson, JR3, CA.

### 3.2.6 Load Cell Tare Load: The Effect of Gravity

Recall that the load cell and fixture rotate with the robot arm. One of the most dramatic effects of this rotation can be seen in the force and moment readings of the JR3 LC as the effect of gravity comes into play. To account for these gravitational effects, the VB program for reading the LC was modified. First, the load cell and the attached fixture weight were measured. Further, the center of rotation for the load cell - fixture assembly was determined (see Figure 3.7). These calculations were incorporated into the load cell reading to cancel out the gravitational effect. Figures 3.8, 3.9, and 3.10 display selected plots of load cell reading before and after the tare load effect.

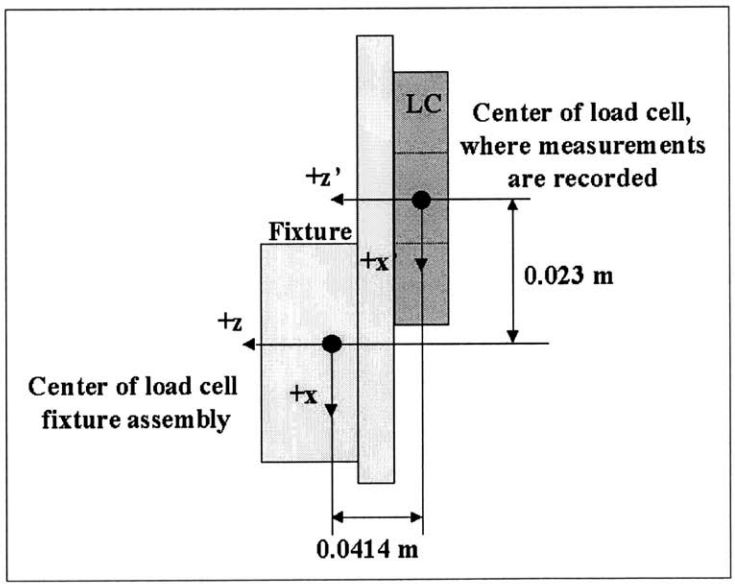


Figure 3.7: Load cell – fixture assembly.

Equations 3.1 and 3.2 describe the general procedure to compensate for the effects (gravitation, and moments) of the fixture assembly on the load cell reading:

$$\vec{F} = \vec{F}_{read\ by\ the\ load\ cell} + \vec{W}_{Load\ cell\ CS} - R_{oat} \cdot \vec{W}_{Global\ CS} \tag{3.1}$$

$$\vec{M} = \vec{M}_{read\ by\ the\ load\ cell} + \vec{m}_{Initial} - \vec{r} \times (R_{oat} \cdot \vec{W}_{Global\ CS}) \tag{3.2}$$

Where:

$\vec{F}$ is a vector (3x1) representing the forces ($F_x$, $F_y$, $F_z$) at any given flexion angle accounting for the gravitational effect of load cell and fixture,

$\vec{F}_{read\ by\ the\ load\ cell}$ is a vector representing the forces (x, y, z) read by the load cell (not including gravitational effect),

$\vec{W}_{Load\ cell\ CS}$ is the weight of the load cell - fixture assembly in load cell coordinate system,

$R_{oat}$ is a 3x3 rotation matrix (zyz sequence) to transform a vector from the global system to the local system (load cell),

$\vec{W}_{Global\ CS}$ is the weight of the load cell - fixture assembly in global coordinate system,

$\vec{M}$ is a vector (3x1) representing the moments ($m_x$, $m_y$, $m_z$) at any given flexion angle accounting for the gravitational effect,

$\vec{M}_{read\ by\ the\ load\ cell}$ is a vector representing the moments ($m_x$, $m_y$, $m_z$) read by the load cell (not including gravitational effect),

$\vec{m}_{Initial}$ is the initial moment read by the load cell due to the fixture assembly, and

$\vec{r}$ is the three dimensional position vector between the load cell center of rotation and the fixture center of rotation written in load cell coordinate system $\vec{r} = [0.023, 0, 0.0414]$ (Figure 3.7).

A VB procedure was written to account for the load cell – fixture assembly gravitational effect for every flexion angle (see Appendix D).

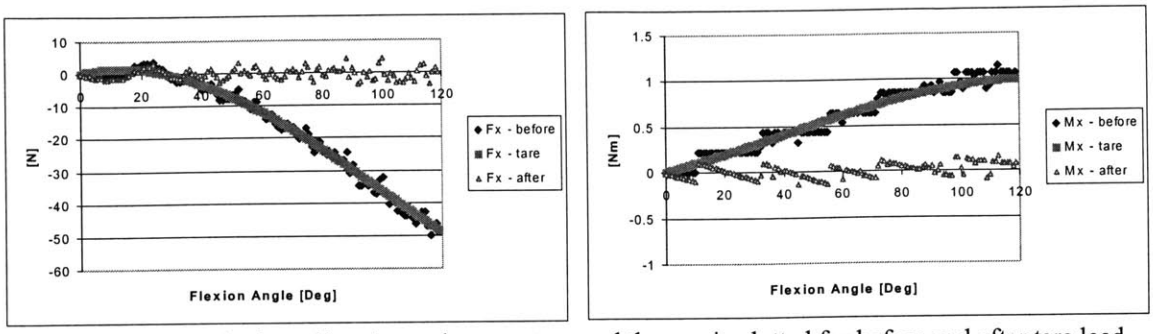


Figure 3.8: Force in the x direction and moment around the x axis plotted for before and after tare load.

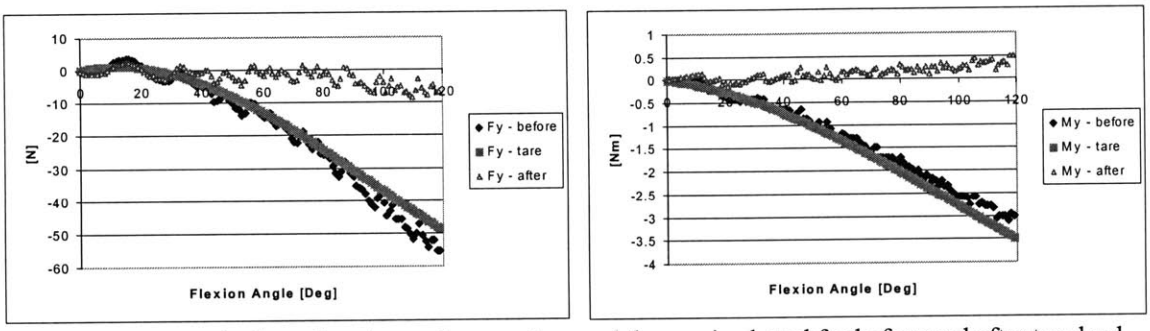


Figure 3.9: Force in the y direction and moment around the y axis plotted for before and after tare load.

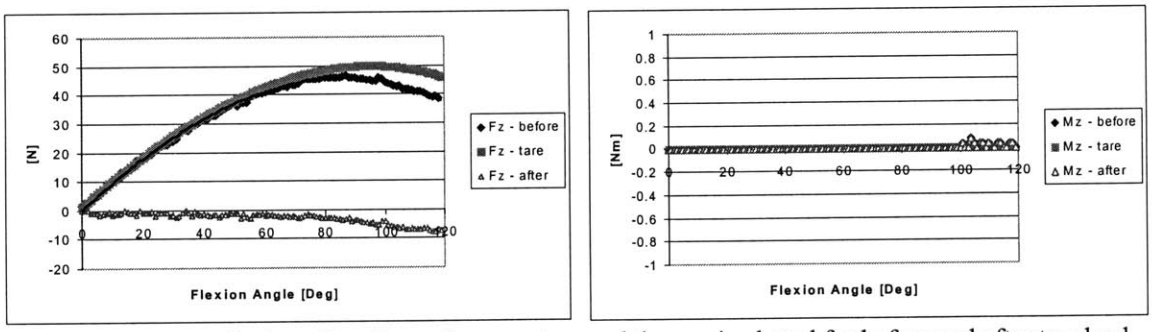


Figure 3.10: Force in the z direction and moment around the z axis plotted for before and after tare load.

## 3.3 Digitization System

Coordinate systems of the knee and of the load cell are required for the calculation of the relative motion of the tibia with respect to the femur. An Immersion MiscroScribe 3DX (Immersion Corporation, CA) digitizer is used to establish these coordinate systems.

The MicroScribe-3DX is a tool for performing 3-dimentional digitizing. Its communication with a PC is done through a standard RS-232 serial port. Figure 3.11 describes the main parts of the MiscroScribe.

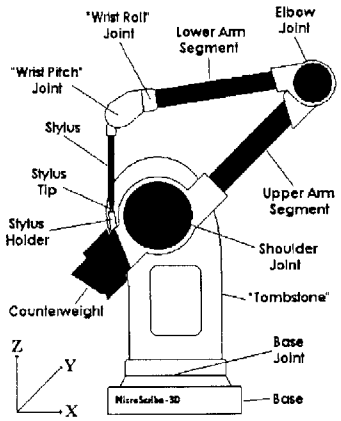


Figure 3.11: MicroScribe parts and features.

The system includes the arm unit, which houses the internal electronics, a serial cable, and an external module. The MicroScribe is connected to COM2 serial port of the PC. A double foot pedal is attached to the rear panel of the digitizing arm for hand-free data selection. The system makes use of five optical sensors to record the relative angles of the device such that the tip location (x, y, and z) is reported. In this project, the stand-alone program called InScribe (developed by Immersion Corporation) was used for data accumulation. This application runs in the background of Windows, entering coordinate values (x, y, and z) directly into Microsoft Excel (V.97). Table 3.3 below lists some of the important features of the MicroScribe-3DX.

Table 3.3: MiscroScribe-3DX selected specification.

| **Workspace** | **Position Accuracy** | **Sampling Rate** |
|---|---|---|
| 1.27m Sphere | 0.23mm | 1000 points/sec |

# Chapter 4

# FORCE AND DISPLACEMENT CONTROLS OF THE TEST SYSTEM

## 4.1 General Description

In the robotic system introduced in Chapter 3, the load cell is rigidly fixed to the end of the robot arm and is free to move with arm motion. The robotic test system controls the position of the knee in space by learning (force control) and replaying (displacement control) predetermined positions of the knee. In this chapter, a detailed description for the development of force and displacement control algorithms for human knee test is presented.

### 4.1.1 Experimental Set-up

In this project, the tibia is mounted on the robotic manipulator through the load cell while the femur is rigidly fixed onto a pedestal. This allows the robot to move the tibia while the femur remains fixed. In this project the knee is placed in an inverted orientation compared to its physiological orientation. Two reasons for this set-up: clinically,

surgeons manipulate the tibia to evaluate TKA stability. Further, the application of muscle loads is done easily when the knee is inverted.

The knee specimen is aligned so that the load cell can measure three force and three moment components along and about a cartesian coordinate system. The longitudinal axis of the tibia (x), the epicondylar (medial-lateral) axis of the femur (y), and the anterior-posterior axis of the knee (z) define the coordinate system (Figure 4.1). The origin of the system is chosen as the midpoint of the trans-epicondylar line.

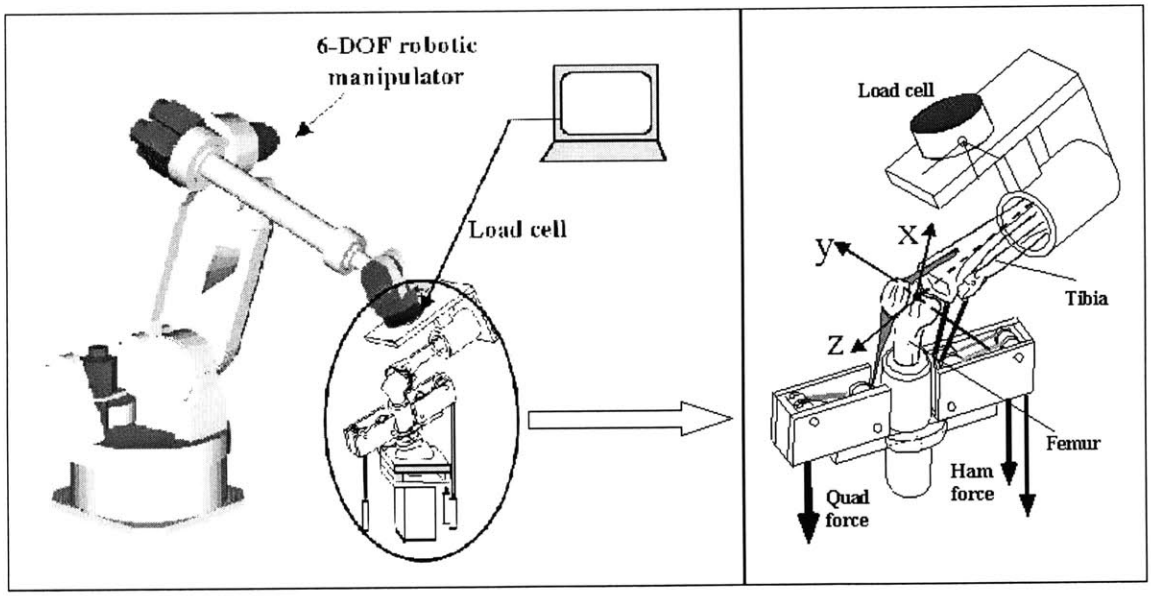


Figure 4.1: Set-up of the robotic testing system

The femoral coordinate system and the tibial coordinate system coincide with each other at full extension of the knee (also called initial position) under no load condition [76]. Thus, only one coordinate system is needed to be defined initially (Figure 4.2a). As the knee responds to external load, the tibial coordinate system moves with the tibia. At that point, the coordinate system of the femur no longer coincides with the coordinate system of the tibia. Therefore, the translation vector and the rotation matrix of the tibia with respect to the femur must be evaluated to determine the knee kinematics (Figure 4.2b).

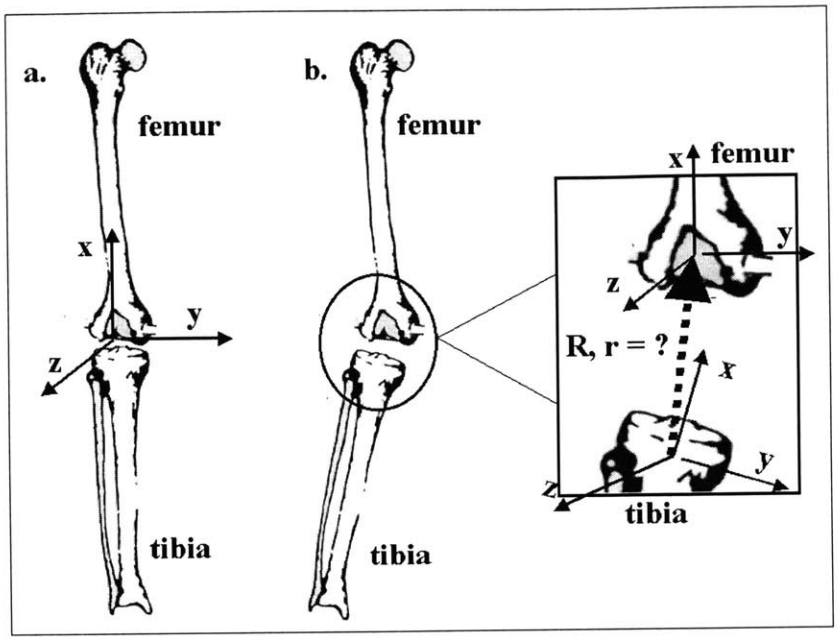


Figure 4.2: Tibia and femur coordinate system (CS) configuration:
a. femur and tibia CS coincide, b. rotated tibia.

There are many ways to construct the initial knee coordinate system (ruler, optical markers, etc.). In this project, the MicroScribe® 3DX, described in section 3.3, was utilized for the digitization of the anatomical points of the knee. These points were then used to reconstruct the knee coordinate system.

### 4.1.2 Coordinate System Development

The knee coordinate system was constructed by digitizing (MicroScribe 3DX®) four anatomic points on the knee (Figure 4.3). Two points parallel to posterior cortex in the longitudinal direction of the tibia (C, D), and midpoints of the insertions of the medial and lateral collateral ligaments (A, B) were specified on the specimen. In addition, the load cell coordinate system was established by digitizing three points ($U_1$, $U_2$, $U_3$) on the load cell.

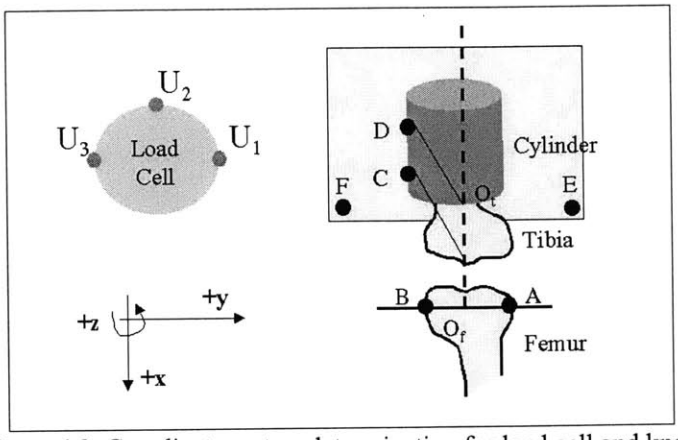


Figure 4.3: Coordinate system determination for load cell and knee.

The knee and load cell axes, as well as their center of rotation were calculated from these digitized points. Table 4.1 presents the major equations involved in these calculations.

Table 4.1: Coordinate system calculations for load cell and knee.

| | Center | x-axis | y-axis | z-axis |
|---|---|---|---|---|
| **Load Cell** | $\vec{O}_u = \frac{\vec{u}_1 + \vec{u}_3}{2}$ | $\vec{O}_u - \vec{u}_2$ | $\vec{u}_1 - \vec{u}_3$ | $\vec{x} \times \vec{y}$ |
| **Knee** | Femur: $\vec{O}_f = \frac{\vec{A} + \vec{B}}{2}$ Tibia: $\vec{O}_t = \vec{O}_f + (\vec{D} - \vec{C})$ | $\vec{O}_f - \vec{O}_t$ | $\vec{A} - \vec{B}$ | $\vec{x} \times \vec{y}$ |

A VB subroutine was written to construct the coordinate system from the digitized points and to calculate the relative rotation ($R_{LK}$) and translation vector ($r_{kl}$) between the knee and the load cell (see Appendix E).

### 4.1.3 Knee-Load Cell-Digitizer Relationship

The relative orientation and translation of the tibia with respect to the femur is of interest. Since the tibia is rigidly fixed to the load cell, the relative orientation and translation of the load cell with respect to the femur are to be measured. Figure 4.4 presents a diagram

relating the digitizer, load cell, and knee. In this section, only the kinematics data is presented. Table 4.2 summarizes the variables involved in this process.

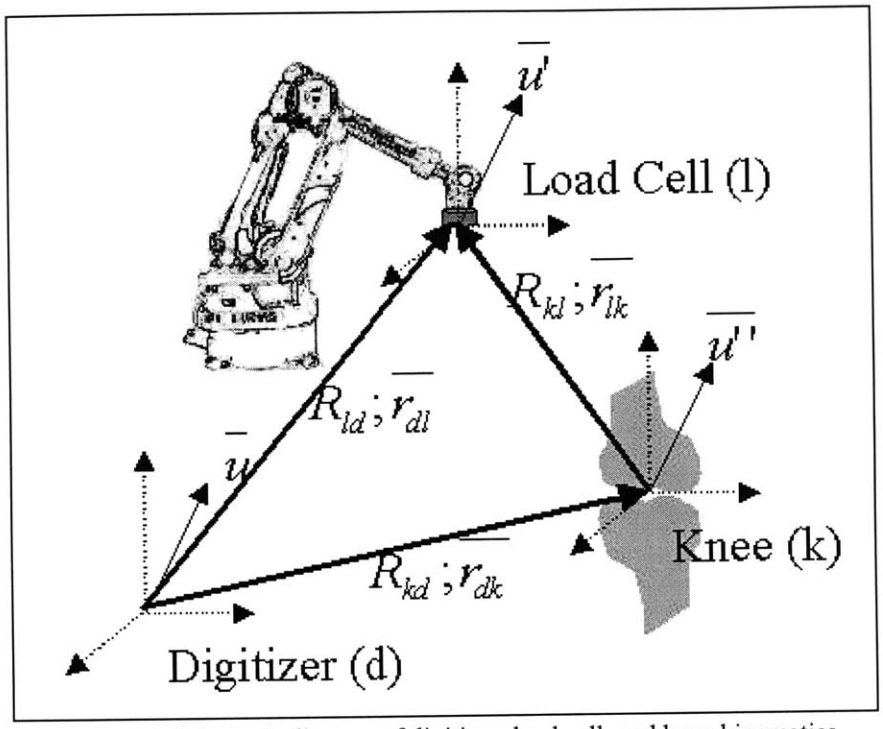


Figure 4.4: Schematic diagram of digitizer, load cell, and knee kinematics.

Table 4.2: Variables description.

| Symbol | Description |
|---|---|
| $\vec{r}_{dk}$ | Translation vector from digitizer to knee |
| $\vec{r}_{dl}$ | Translation vector from digitizer to LC |
| $\vec{r}_{lk}$ | Translation vector from LC to knee |
| $R_{kd}$ | Rotation matrix of knee relative to digitizer |
| $R_{ld}$ | Rotation matrix of LC relative to digitizer |
| $R_{kl}$ | Rotation matrix of knee relative to LC |

The following VB code was written to construct the translation vector $\vec{r}_{dk}$ and the rotation matrix $R_{kd}$:

```
'read the points A, B, C, D, and E from a tab delineated file
Input #11, Ax, Ay, Az, Bx, By, Bz, Cx, Cy, Cz, Dx, Dy, Dz, Ex, Ey, Ez, Fx, Fy, Fz
'calculating center of rotation for the femur
Ofx = (Ax + Bx) / 2
```

```
Ofy = (Ay + By) / 2
Ofz = (Az + Bz) / 2
'calculating center of rotation for the tibia
Otx = Ofx + (Dx - Cx)
Oty = Ofy + (Dy - Cy)
Otz = Ofz + (Dz - Cz)
'calculating the orthonormal basis for femur
'assume femur and tibia CS coincide
'*****
'horizontal matrix
'*****
'x axis
Rkd(1, 1) = (Ofx - Otx) / Sqr((Ofx - Otx) ^ 2 + (Ofy - Oty) ^ 2 + (Ofz - Otz) ^ 2)
Rkd(1, 2) = (Ofy - Oty) / Sqr((Ofx - Otx) ^ 2 + (Ofy - Oty) ^ 2 + (Ofz - Otz) ^ 2)
Rkd(1, 3) = (Ofz - Otz) / Sqr((Ofx - Otx) ^ 2 + (Ofy - Oty) ^ 2 + (Ofz - Otz) ^ 2)
'y axis
Rkd(2, 1) = (Ax - Bx) / Sqr((Ax - Bx) ^ 2 + (Ay - By) ^ 2 + (Az - Bz) ^ 2)
Rkd(2, 2) = (Ay - By) / Sqr((Ax - Bx) ^ 2 + (Ay - By) ^ 2 + (Az - Bz) ^ 2)
Rkd(2, 3) = (Az - Bz) / Sqr((Ax - Bx) ^ 2 + (Ay - By) ^ 2 + (Az - Bz) ^ 2)
'z axis
Rkd(3, 1) = Rkd(1, 2) * Rkd(2, 3) - Rkd(2, 2) * Rkd(1, 3)
Rkd(3, 2) = Rkd(1, 3) * Rkd(2, 1) - Rkd(2, 3) * Rkd(1, 1)
Rkd(3, 3) = Rkd(1, 1) * Rkd(2, 2) - Rkd(1, 2) * Rkd(2, 1)
'normalized z
Rkd_norm = Sqr(Rkd(3, 1) ^ 2 + Rkd(3, 2) ^ 2 + Rkd(3, 3) ^ 2)
Rkd(3, 1) = Rkd(3, 1) / Rkd_norm
Rkd(3, 2) = Rkd(3, 2) / Rkd_norm
Rkd(3, 3) = Rkd(3, 3) / Rkd_norm

'y cross z = x to ensure all are orthonormal
Rkd(1, 1) = Rkd(2, 2) * Rkd(3, 3) - Rkd(3, 2) * Rkd(2, 3)
Rkd(1, 2) = Rkd(2, 3) * Rkd(3, 1) - Rkd(3, 3) * Rkd(2, 1)
Rkd(1, 3) = Rkd(2, 1) * Rkd(3, 2) - Rkd(2, 2) * Rkd(3, 1)
```

Similar codes were developed for $\vec{r}_{dl}$ translation vector and $R_{ld}$ rotation matrix (Appendix E). Finally, the relative motion between the load cell and the knee can be calculated by using rigid body motion equations. The translation vector, $\vec{r}_{kl}$ , between the load cell and the knee can be calculated by:

$$\vec{r}_{kl} = \vec{r}_{dl} - \vec{r}_{dk} \,. \tag{4.1}$$

The orientation of the knee relative to the load cell, $R_{lk}$, can be derived by a series of transformation. Let us look at a vector $\vec{u}$, which is located in the digitizer CS (Figure 4.4). We can transform the vector $\vec{u}$ to the $\vec{u}'$ (load cell) CS via two routes: (1)

clockwise, i.e. going form the digitizer to the load cell, knee and back to the beginning, or (2) counter-clockwise, starting from the digitizer, going through the knee, load cell, and back to the digitizer. Both paths should be equal to each other. Let us start with the first method. The transformation of vector $\vec{u}$ to the $\vec{u}'$ can be done by using the rotation matrix $R_{ld}$ (i.e. rotation matrix of LC relative to digitizer).

$$\vec{u}' = R_{ld} \cdot \vec{u} \,. \tag{4.2}$$

We can now look at the second method and transform vector $\vec{u}$ to $\vec{u}''$ system (knee system):

$$\vec{u}'' = R_{kd} \cdot \vec{u} \,. \tag{4.3}$$

We can take it one further step, and transform vector $\vec{u}''$ in the knee system to the load cell system ($\vec{u}'$) using $R_{lk}$ transformation matrix. Finally we can use equations 4.2 and 4.3 to relate vector $\vec{u}$ to the $\vec{u}'$:

$$\vec{u}' = R_{lk} \cdot \vec{u}'' = R_{lk} \cdot R_{kd} \cdot \vec{u} \,. \tag{4.4}$$

From equations 4.2-4.4 we need to solve for the rotation of the tibia with respect to the femur ($R_{lk}$):

$$R_{ld} = R_{lk} \cdot R_{kd} \Rightarrow R_{lk} = R_{lk} \cdot R_{kd}^{\,T} \,. \tag{4.5}$$

### 4.1.4 Robot-Knee-Load Cell Relationship

In this protocol, each element (robot manipulator, load cell, tibia and femur) of the system is represented by an arbitrary coordinate system. The robot base is fixed to the floor and will be denoted as the global coordinate system. The femur is rigidly fixed to the floor (via a pedestal). The tibia is free to move with the load cell and the robot

manipulator and therefore, their coordinate systems are rigidly fixed relative to each other. Figure 4.5 graphically presents the setup of the four elements.

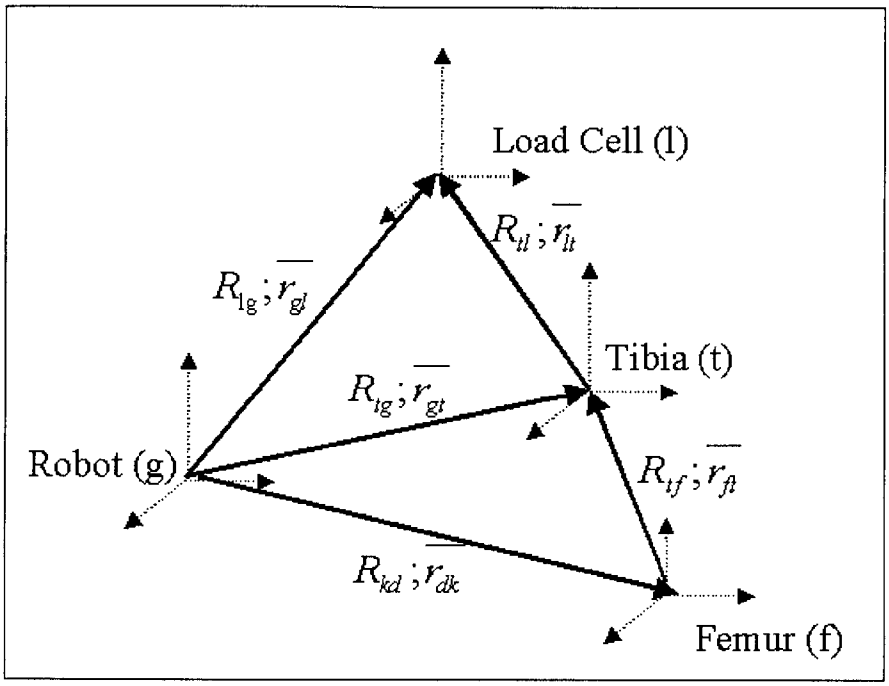


Figure 4.5: Graphic representation of the four coordinate systems.

Table 4.3 below summarizes the variables involved in this protocol. Table 4.4 summarizes all the known and unknown variables involved in this process.

Table 4.3: Variables summary.

| Symbol | Interpretation |
|---|---|
| t | Tibia |
| f | Femur |
| l | Load Cell |
| g | Global (Robot Base) |
| $\bar{r}$ | Translation vector |
| R | Rotation matrix |

Table 4.4: List of known and unknown variables.

| Symbol | Description | Known/Unknown |
|---|---|---|
| $\vec{r}_{gf}$ | Translation vector of from robot to femur | Known and fixed at all time |
| $\vec{r}_{tl}$ | Translation vector of tibia to load cell | Fixed at all times |
| $\vec{r}_{gl}$ | Translation vector of robot to load cell | Calculated for every flexion angle |
| $\vec{r}_{ft}$ | Translation vector of femur to tibia | Unknown |
| $R_{fg}$ | Rotation matrix of femur around global system | Known and fixed at all time |
| $R_{lt}$ | Rotation matrix of tibia around load cell | Directly measured and calculated |
| $R_{lg}$ | Rotation matrix of global about load cell | Calculated for every flexion angle |
| $R_{tf}$ | Rotation matrix of femur about tibia | Unknown |

The procedure for calculating an unknown rotation matrix and a translation vector for a sequence of transformation is outlined in section 4.1.3. Equations 4.6 and 4.7 represent the final results for the translation vector, $\vec{r}_{ft}$, and the rotation matrix, $R_{tf}$, respectively:

$$\vec{r}_{ft} = \vec{r}_{gl} - \vec{r}_{tl} - \vec{r}_{gf} \tag{4.6}$$

$$R_{ft} = R_{lt}^{\ T} \cdot R_{lg} \cdot R_{fg}^{\ T}. \tag{4.7}$$

These variables, $\vec{r}_{ft}$ and $R_{ft}$, represent the position and orientation of the tibia with respect to the femur, respectively.

## 4.2 Force Control Algorithm

In this section, a newly developed mathematical approach for the investigation of non-linear coupled mechanical characteristics of the human knee joint under external loading conditions is introduced. This algorithm has been used as the basis of force control of the robotic test system.

The objective of force control mode is to find an equilibrium position of the knee corresponding to specific loads. Thus, when operating in force control mode, the robot applies a specific force to the knee joint that causes movement to a new location relative to the location prior to loading. The force transmitted through the knee balances the external load applied to the knee:

$$\vec{f}_{external} - \vec{F}(\vec{x})_{internal} = 0 \tag{4.8}$$

The external force is a derived value. The internal equivalent force, $\vec{F}(\vec{x})$, is the constraint forces of the knee components such as ligaments, cartilage, and bony contact. In order to find the knee position $\vec{x}$ under external loads, the above equation has to be solved.

In this project, a Quasi-Newton method (Broyden's method) is utilized to solve the above equation [77]. Broyden's method is based on Newton-Raphson global convergence method [78]. Derivation of Broyden's method can be found in Appendix F.

### 4.2.1 Use of Broyden's Method in the Control Algorithm

In the force control mode, the load cell measures the load transferred through the knee joint $\vec{F}^{knee}(\vec{x},\theta)$, where $\vec{x}$ represents the position vector ($x$ $y$, $z$) and $\theta$ represents the three Euler angles ($o$, $a$, $t$) of the tibia rotation with respect to the femur. As mentioned earlier, the convention of the Euler sequence used in this project is $y$-$z$-$x$ that means a rotation sequence of flexion/extension rotation followed by internal/external rotation followed by varus/valgus rotation. The $\vec{x}$ and the $\theta$ express the knee position in space relative to the robot base (global CS). The load $\vec{F}^{knee}$ has six components: three force

components ($f_x^{knee}, f_y^{knee}, f_z^{knee}$) and three moment components ($m_x^{knee}, m_y^{knee}, m_z^{knee}$). The difference of the target load and the load measured by the load cell is expresses by:

$$\vec{F}(\vec{x},\theta) = \vec{F}^{Target} - \vec{F}^{knee}(\vec{x},\theta) \tag{4.9}$$

where $\vec{F}(\vec{x},\theta)$ is an implicit function of the knee position, measured by the robotic system. In order to reach an equilibrium position, an iteration procedure is adopted in the test system. Equation 4.9 can be written in terms of the *i*th iteration. This denotes the difference of the target load and the load measured by the load cell at the *i*th iteration:

$$\vec{F}(\vec{x}_i,\theta_i) = \vec{F}^{Target} - \vec{F}^{knee}(\vec{x}_i,\theta_i) \tag{4.10}$$

Convergence criteria for both forces and moments is used for the equilibrium position of the knee:

$$\begin{aligned} |\vec{f}| &\le \varepsilon_f \\ |\vec{m}| &\le \varepsilon_m \end{aligned} \tag{4.11}$$

where $\vec{f}$ represents the three force components of $\vec{F}(\vec{x},\theta)$, $\vec{m}$ represents the three moment components of $\vec{F}(\vec{x},\theta)$, $\varepsilon_f = 3\,\text{N}$, and $\varepsilon_m = 0.5\,\text{Nm}$ [76, 79, 80]. If $\vec{F}(\vec{x}_i,\theta_i)$ does not satisfy the above convergence criteria, the robot moves the knee joint to a new location by an incremental displacement $\Delta\vec{a}_i$ which includes three incremental translation components ($\Delta\vec{x}_i$) and three incremental angular components ($\Delta o_i, \Delta a_i, \Delta t_i$). This incremental displacement $\Delta\vec{a}_i$ can be derived using Broyden's method [77]:

$$\Delta\vec{a}_i = -B_i^{-1}\cdot\vec{F}(\vec{x}_i\theta_i) \tag{4.12}$$

where $B_i^{-1}$ is the inverse Jacobian matrix representing the 6x6 incremental stiffness matrix of the knee that takes into account the coupling effect of different degrees of freedom of the knee joint. $B_i^{-1}$ can be written as follows:

$$B_i^{-1} = B_{i-1}^{-1} + \frac{(\Delta \vec{a}_{i-1} - B_{i-1}^{-1} \cdot \Delta \vec{F}_{i-1}) \otimes \Delta \vec{a}_{i-1} \cdot B_{i-1}^{-1}}{\Delta \vec{a}_i \cdot B_{i-1}^{-1} \cdot \Delta \vec{F}_{i-1}} \quad i \geq 1 \tag{4.13}$$

where $\Delta \vec{F}_{i-1} = \vec{F}(x_i, \theta_i) - \vec{F}(x_{i-1}, \theta_{i-1})$ and $\otimes$ represents the tensor product of two vectors. At first iteration ($i$=1), an initial approximation, $B_0$, is adopted as a diagonal matrix [81]. After the robot moves the tibia to a new position, the load cell measures the forces and moments transferred through the knee joint. Convergence criteria is evaluated again (equation 4.10). This process of iteration continues until the convergence criteria are satisfied.

### 4.2.2 Application of Broyden's Method in Finding the Neutral Path of a Human Knee Joint

The initial position of the knee at any flexion angle is crucial for measuring joint kinematics (motion) or kinetics (such as measuring ligament force in response to external loads). This initial position provides the system with a reference configuration to which all other measurements can be compared. The neutral path is the path that passes through the neutral position points. A neutral position point is defined as the position of the knee where the knee carries minimal load under no external load. For the knee joint, we determine the neutral path from fully extended knee to 120 degrees of flexion. To determine the neutral position using the robotic test system, the target force $\vec{F}^{Target}$ is set to zero. The overall procedure for finding a neutral path for a given knee is outlined in

Figure 4.6. The flow chart describes the steps involved in the process of finding the neutral path of a given human knee specimen.

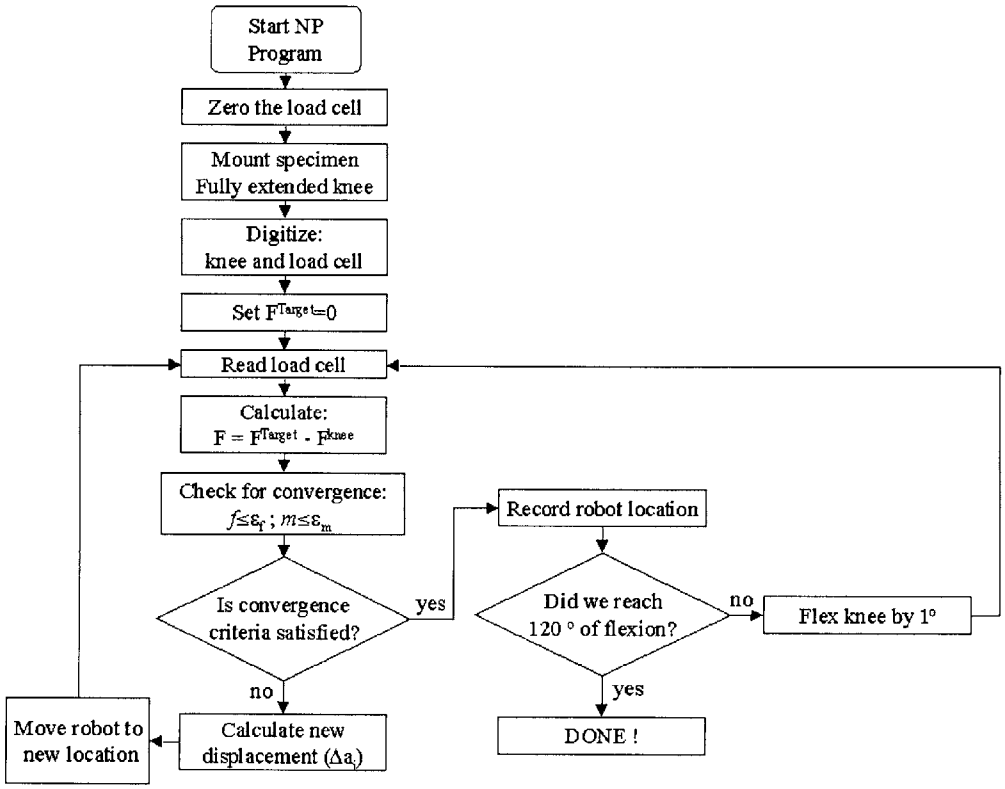


Figure 4.6: Flow chart describing neutral path (NP) determination.

## 4.3 Displacement Control Mode

The objective of this operational mode is to find the forces and moments corresponding to a specific location of the knee. In this position control mode, the robot moves the specimen to a given location. At the end of robot motion, the load cell reads the forces and moments associated with that particular position. These forces and moments are used for kinetics analysis.

## 4.4 Application of the System for Measuring Ligament Force.

This section illustrates how the testing system is suitable for measuring ligaments force (such as PCL) of the knee when the knee is subjected to external loads at a fixed flexion angle. Once the neutral path of a given specimen is determined, external load is applied to the knee specimen. The tibia moves in the remaining 5-DOF (flexion angle is constraint in this project) until reaching an equilibrium position. The equilibrium position is defined as the position where the external load and the constraint forces of the knee (i.e. joint contact, ligament force, etc.) are balanced. This equilibrium position represents the kinematics changes of the knee in response to the applied external load. The PC records this position and the load cell measures the residual forces. A residual force is the difference between the external load and the constraint force at the equilibrium position that satisfy the convergence criteria (equation 4.10). To determine the PCL forces, the PCL is transected. The robot then returns the knee back to the equilibrium positions using position control mode. The load cell measures the corresponding forces ( $\vec{F}_d$ ) required to maintain this equilibrium position in the absence of the PCL. Using the principle of superposition (assume rigid bony structure), the difference between the two forces (measured before and after PCL transaction) represents the PCL force under external loading conditions [61, 79, 80]:

$$\vec{F}_{PCL} = \vec{F}_i - \vec{F}_d . \tag{4.14}$$

## 4.5 Significance of the System

Total knee arthroplasty (TKA) has been a popular operation for people with severe degenerative joint disorders such as OA. One of the major purposes of TKA is to restore normal knee function, i.e. knee range of motion and force transmission through the knee joint. It is desired to test the same knee specimen for its intact as well as TKA biomechanical response to objectively evaluate the function of the TKA. This information will be significant for further improvement of TKA as well as surgical procedures.

The robotic testing system, developed in this project is able to test intact, injured, and reconstructed knee specimens. This system provides both displacement and force control capabilities, and is able to determine knee joint motion under simulated muscle loads and other external loading conditions. This system defines the intact knee biomechanics and uses this information to evaluate the efficiency of total knee replacement in the restoration of normal knee function. The key advantage of this system is the capability to limit intra-specimen variation by performing multiple tests on the same knee specimen. The system sets quantitative guidelines for the effectiveness of current surgical treatments in the restoration of normal knee biomechanical functions. This system is readily applicable for biomechanical studies of various musculoskeletal joints.

# Chapter 5

# DETERMINATION OF TKA KINEMATICS USING THE ROBOTIC SYSTEM

In the previous chapters, a robotic test system for evaluating various TKAs was introduced. This test system is used for functional evaluation of TKAs using the native specimen as the comparative model. In this chapter, kinematics data of two human knee specimens, obtained from the same donor (right and left knee), was collected using the robotic test system. Following intact knee kinematics measurement, each knee was surgically treated using a typical TKA, and the kinematics of the TKA knee was measured under the identical loading conditions. A second and third TKA were performed, successively on the same specimen. Three typical TKA prostheses were examined:

I. Posterior cruciate retaining (PCR)

II. Posterior cruciate sacrificing (PCSac)

III. Posterior cruciate substitution (PCSub)

## 5.1 Basis for Interpretation

Neutral position for each TKA was determined and compared to the neutral position of the native knee to examine the changes in knee kinematics (protocol described in section 4.2.2). The data presented here demonstrates the capability of the robotic testing system for TKA application in biomechanics. Throughout the testing protocol the femur was rigidly fixed while the tibia was free to move with the robot arm. Tibia motion relative to femur (Figure 5.1) was measured by the robotic system. At the beginning of the experiment, an orthogonal coordinate system was fixed to the femur (X-Y-Z) and to the tibia (x-y-z). Initially (i.e. knee at full extension), the femur and tibia coordinate systems coincide. At each flexion angle (along the femur Y axis), tibial motion was determined by its relative position to the femur. Tibia translation and orientation with respect to the femur were evaluated at every flexion angle from fully extended knee to 120 degrees flexion. The tibial rotation was expressed in an Euler series, Y-Z-X, where the three angles in this series are *O, A, T.*

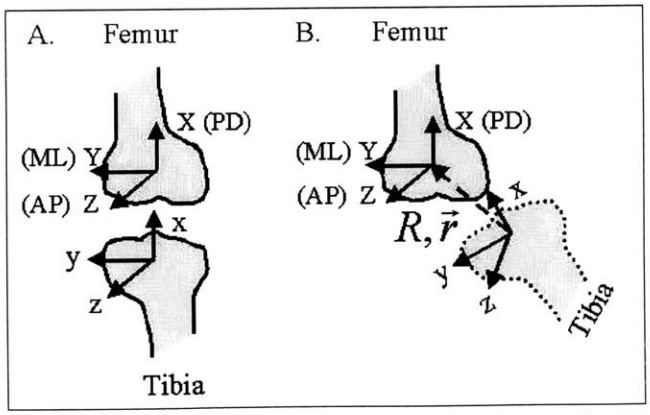


Figure 5.1: Knee coordinate system establishment; A. Knee at full extension, B. Knee after a given translation and a rotation (ML: medial lateral translation, AP: anterior posterior translation; PD: proximal distal translation).

## 5.2 Translation Data

Figures 5.2 to 5.7 display tibial translation with-respect-to the femur at every flexion angle throughout the full neural path range of motion. Tibial translation of the native knee in the negative X-direction (Figures 5.2, 5.3) appears to be larger than TKAs translation, for both the right and the left knee.

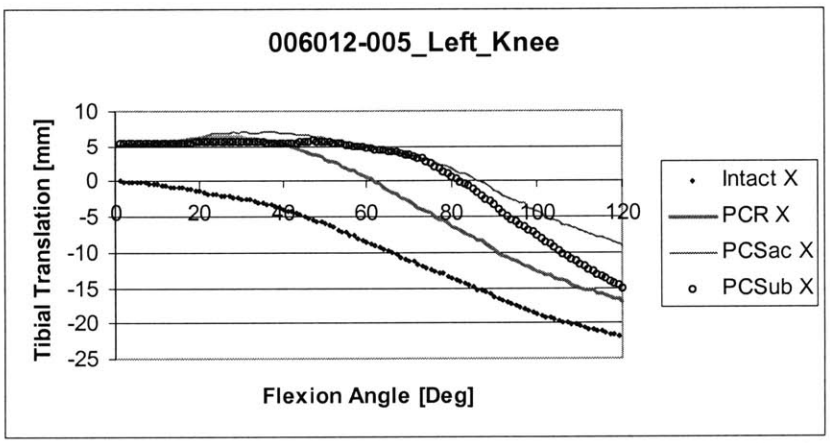


Figure 5.2: Tibial translation with-respect-to femur CS in the X-direction (left knee).

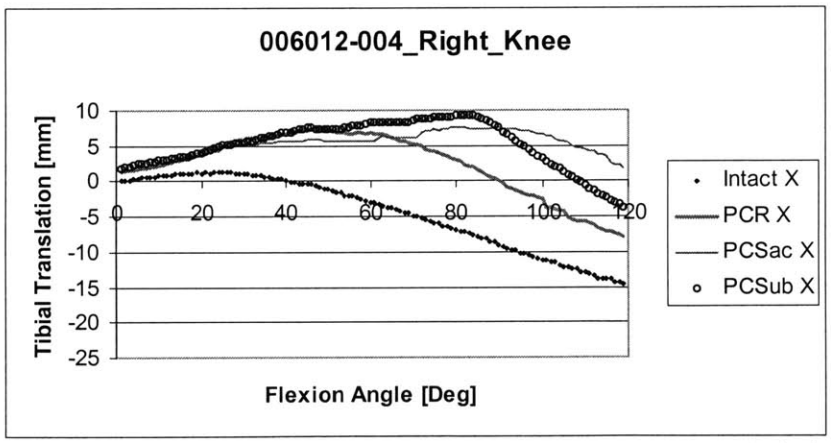


Figure 5.3: Tibial translation with-respect-to femur CS in the X-direction (right knee).

Similarly, tibial translation in the Y-direction of the native knee is larger than the TKAs Y-tibial translation. However, the magnitude of the tibial translation of the left knee is greater than that of the right knee (Figures 5.4, 5.5).

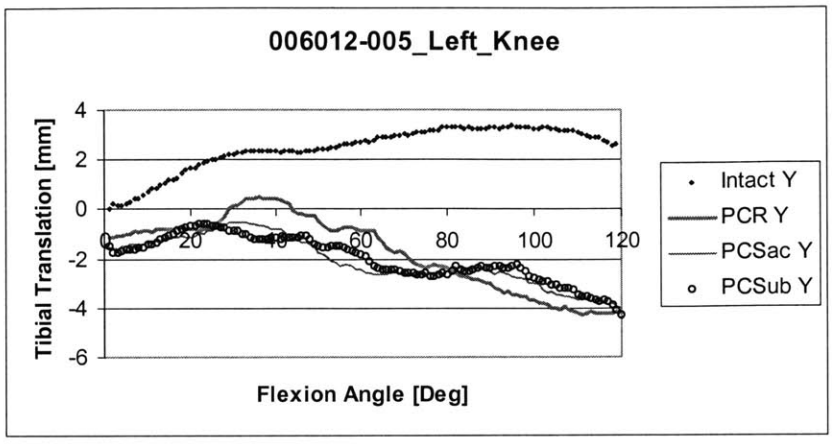


Figure 5.4: Tibial translation with-respect-to femur CS in the Y-direction (left knee).

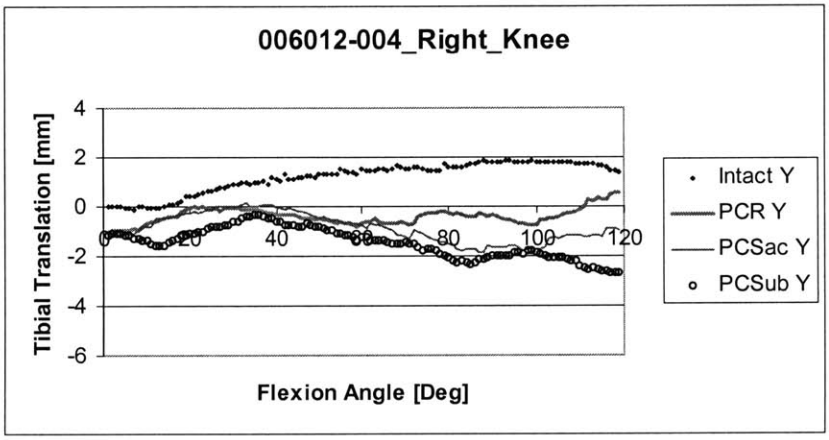


Figure 5.5: Tibial translation with-respect-to femur CS in the Y-direction (right knee).

For low flexion angles, the Z-tibial translation of the intact knee differs from TKAs. However, this difference becomes smaller at higher flexion angles (Figures 5.6, 5.7).

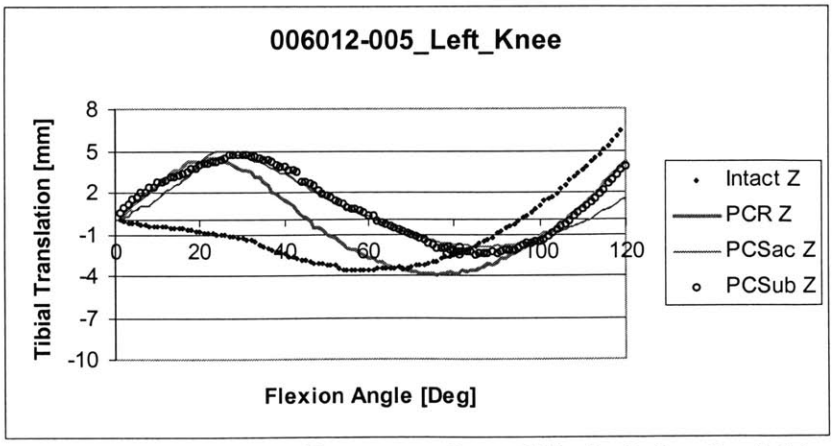


Figure 5.6: Tibial translation with-respect-to femur CS in the Z-direction (left knee).

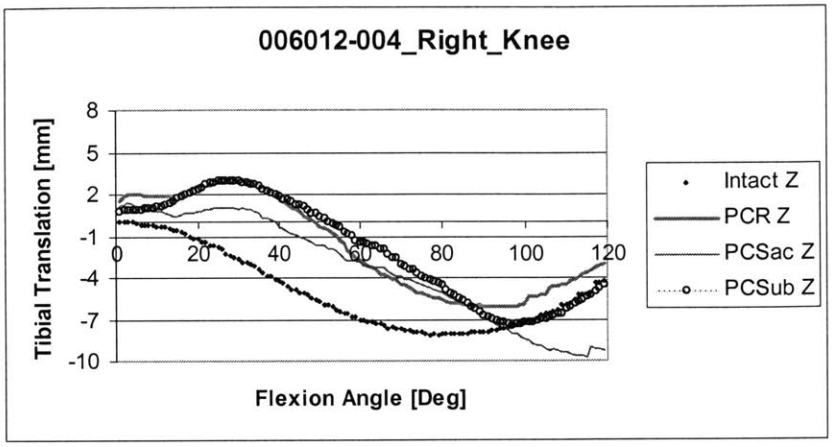


Figure 5.7: Tibial translation with-respect-to femur CS in the Z-direction (right knee).

## 5.3 Rotation Data

Figures 5.8 to 5.11 display tibial rotation with-respect-to the femur at every flexion angle throughout the full neutral path range of motion. From these graphs it appears that the intact knee rotations are similar to the TKAs rotations through the entire range of motion.

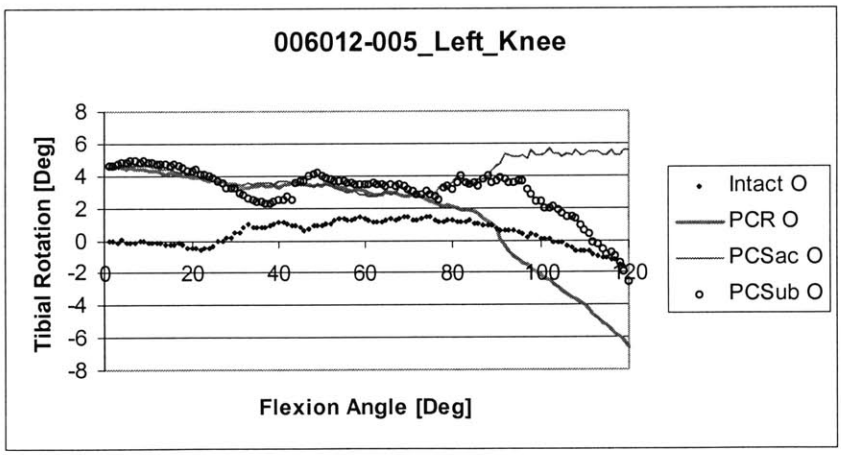


Figure 5.8: Tibial rotation with-respect-to X-axis of femur CS (left knee).

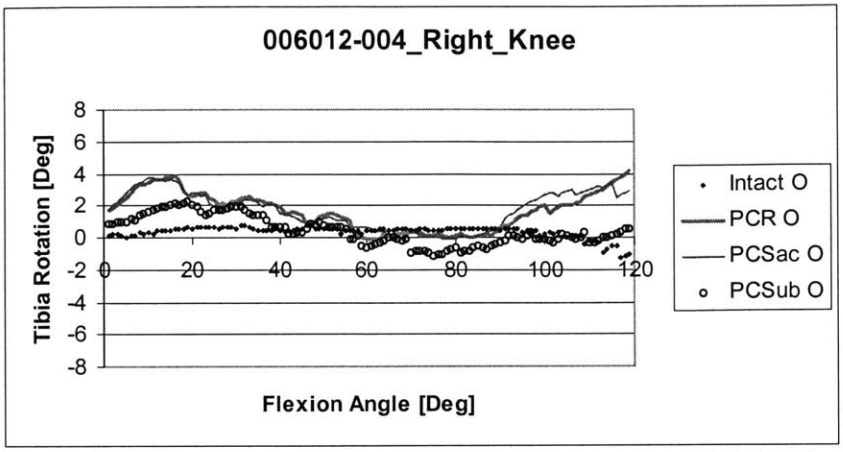


Figure 5.9: Tibial rotation with-respect-to X-axis of femur CS (right knee).

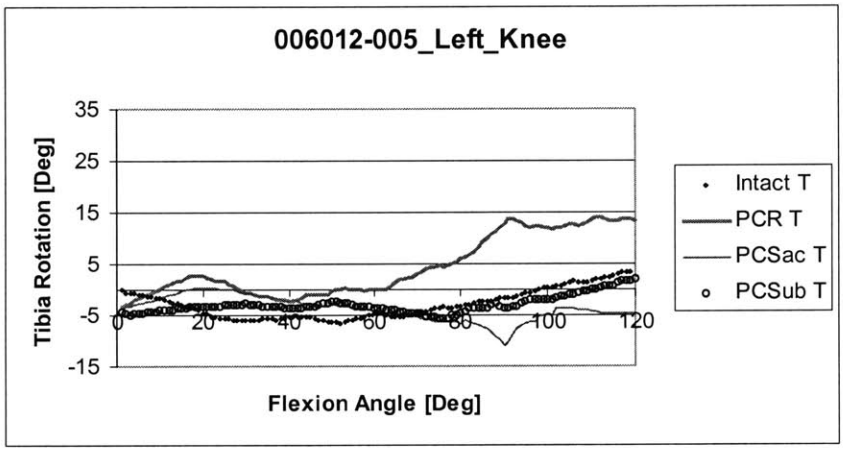


Figure 5.10: Tibial rotation with-respect-to Z-axis of femur CS (left knee).

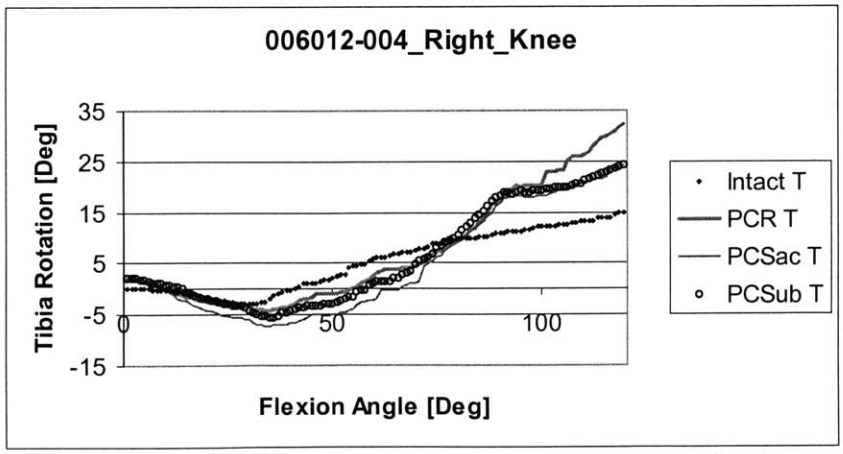


Figure 5.11: Tibial rotation with-respect-to Z-axis of femur CS (right knee).

## 5.4 Analysis and Conclusions

The preliminary results reveal that the neutral path of each TKA implant, used in this study, closely follows the native knee neutral path in rotation. Discrepancies in translation between the TKAs and the intact knee are apparent. The increase seen in the graphs at zero degree of flexion illustrates the difference in the knee position pre and post TKA procedure. During the surgical TKA procedure, bone is removed to fit the implant. In addition, a polyethylene (PE) liner is inserted between the femur and the tibia metal plates. The selection of the implant and the PE liner is performed subjectively by the surgeon based upon guidelines supplied by the implant manufacturer. The TKA components cannot restore the native knee geometry, thus, causing this change in the initial knee position.

There are two ways to evaluate the TKA data. First, comparing the data for each TKA, it is evident that the shape of all TKA curves (PCR, PCSac, and PCSub) are comparable to the shape of the intact knee curve, throughout the full range of motion. Second, when comparing the TKA curves against one another at low flexion angles ( <60 degrees), the TKA curves appear to follow each other closely. However, as flexion angle increases above 60 degrees, the TKA curves, in most cases, diverge and the differences among the TKAs become noticeable.

The results presented here demonstrate the capability of the robotic system for studying the biomechanics of TKA. It is shown that the system is capable of characterizing knee kinematics for both the native human knee and the TKA knee. The advantages of this system are repeatability, non-contact measurements, and capability to

limit intra-specimen variation by performing multiple tests on the same knee specimen (intact knee, knee after various surgical modification, etc.). Future studies will include various kinematics aspects of the knee under external loads. Joint contact pattern as well as soft tissue tension post-TKA will be investigated. An optimal design protocol for TKA will be pursued. The goal of this protocol will be to restore intact knee kinematics and constraint forces of tissue components inside the knee joint. The system could be further modified to determine optimal designs of various artificial joint replacements, using normal joint biomechanics as an objective function.

# Appendix A

# RIGID BODY MOTION USED IN THIS PROJECT

Throughout the development of the control algorithm for the robotic manipulator it was clear that researchers use different mathematical representations for the motion description. Therefore, the notations and the symbols used in this work are presented here. Further, the fundamental equations that govern kinematics and their solutions are derived in this appendix.

## A.1 Position Vector and Rotation Matrix

The robotic manipulator can be modeled as a system of rigid bodies. The motion of a rigid body has six degrees of freedom: three translations and three rotations (orientation). A position vector and a rotation matrix can be used to describe each location of a given robotic joint at a given time. It is necessary to establish a coordinate system and a point in space to describe a position vector (Figure A.1). In this thesis, vectors are written in the form of: $\vec{r}_{AB} = \vec{r}_{A\to B} = \vec{r}_B - \vec{r}_A$ which describes the position vector $\vec{r}$ from point A to point B.

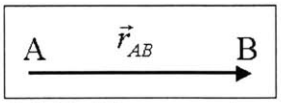


Figure A.1: Position vector description.

To represent the orientation of a given rigid body, three axes are attached to the rigid body (Figure A.2).

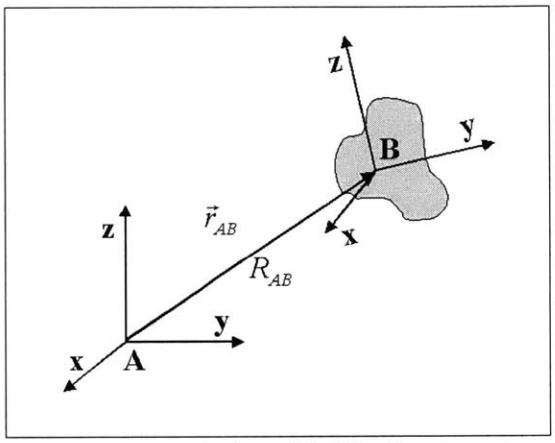


Figure A.2: Description of rigid body orientation.

$R_{AB}$ 3×3 rotation matrix describes the orientation of body B observed from body A (i.e. rotation from A to B). Each component of $R_{AB}$ rotation matrix (cosine matrix) can be written as the dot product of a pair of unit vectors:

$$R_{AB} = \begin{bmatrix} X_B \cdot X_A & Y_B \cdot X_A & Z_B \cdot Z_A \\ X_B \cdot Y_A & Y_B \cdot Y_A & Z_B \cdot Y_A \\ X_B \cdot Z_A & Y_B \cdot Z_A & Z_B \cdot Z_A \end{bmatrix} \quad \text{(A.1)}$$

Where:

$X_A$, $Y_A$, $Z_A$ are unit vectors giving the principle directions for coordinate system A

$X_B$, $Y_B$, $Z_B$ are unit vectors giving the principle directions for coordinate system B.

Note that the transpose of the $R_{AB}$ rotation matrix can give the relative rotation of A with respect to (wrt) B, i.e. $R_{AB}= R_{BA}^T$. The rotation matrix is orthogonal and therefore, $R_{AB}^T= R_{AB}^{-1}$ [82].

## A.2 Euler Angles

From classical mechanics, the orientation of a body can be define by a set of three angles (Euler angles) , which describe the orientation of a set of axes fixed in the rigid body (local coordinate) with respect to a reference axes (global coordinate) [83]. The component of a free vector rotating about its Z axis can be obtained geometrically (Figure A.3):

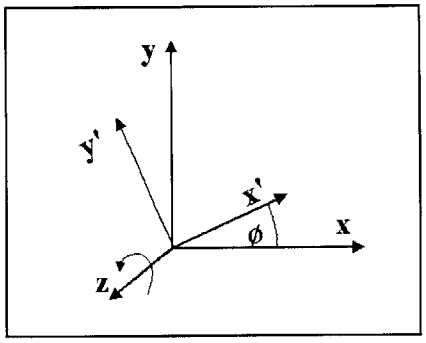


Figure A.3: Rotation about the Z-axis of a reference frame.

$$x' = x \cdot \cos\phi + y \cdot \sin\phi \tag{A.2}$$
$$y' = -x \cdot \sin e\phi + y \cdot \cos\phi$$
$$z' = z$$

$$\begin{bmatrix} x' \\ y' \\ z' \end{bmatrix} = \begin{bmatrix} \cos\phi & \sin\phi & 0 \\ -\sin\phi & \cos\phi & 0 \\ 0 & 0 & 1 \end{bmatrix} \begin{bmatrix} x \\ y \\ z \end{bmatrix} \tag{A.3}$$

The rotation matrix about the Z axis is the 3X3 matrix relating the two different reference frames x, y, z and x', y', z'.

$$R_Z = \begin{bmatrix} \cos\phi & \sin\phi & 0 \\ -\sin\phi & \cos\phi & 0 \\ 0 & 0 & 1 \end{bmatrix} \tag{A.4}$$

The same method can be applied to the rotation about the x and y axis, respectively:

$$\begin{bmatrix} x' \\ y' \\ z' \end{bmatrix} = \begin{bmatrix} 1 & 0 & 0 \\ 0 & \cos\psi & \sin\psi \\ 0 & -\sin\psi & \cos\psi \end{bmatrix} \begin{bmatrix} x \\ y \\ z \end{bmatrix} \tag{A.5}$$

$$R_x = \begin{bmatrix} 1 & 0 & 0 \\ 0 & \cos\psi & \sin\psi \\ 0 & -\sin\psi & \cos\psi \end{bmatrix} \tag{A.6}$$

$$\begin{bmatrix} x' \\ y' \\ z' \end{bmatrix} = \begin{bmatrix} \cos\theta & 0 & -\sin\theta \\ 0 & 1 & 0 \\ \sin\theta & 0 & \cos\theta \end{bmatrix} \begin{bmatrix} x \\ y \\ z \end{bmatrix} \tag{A.7}$$

$$R_y = \begin{bmatrix} \cos\theta & 0 & -\sin\theta \\ 0 & 1 & 0 \\ \sin\theta & 0 & \cos\theta \end{bmatrix} \tag{A.8}$$

These three matrices for the rotation about a particular coordinate axes are essential in the development of Eulerian angles. We can take this one step further and perform successive rotations to transform a vector from one coordinate system to another. The sequence of multiplication of these rotation matrices is crucial because different sequences will result in a different description (angles) of the same rotation. In this project, two main sequences were of interest: (1) ZYZ sequence, and (2) YZX sequence. The former represents the orientation angles by the robotic system. The later, ease in the calculations of knee kinematics (Y-flexion/extension; Z-verus/valgas; X-internal/ external rotation).

We have already introduced the rotation matrices and we mentioned that the sequence of multiplication is important. The question now is how do we determine the desired sequence. It is always a good idea to start from the basic definitions. Looking at

a simple example, Figure A.4 presents a step-by-step transformation of a vector $\vec{u}$ (frame A) to vector $\vec{u}'''$ (frame B).

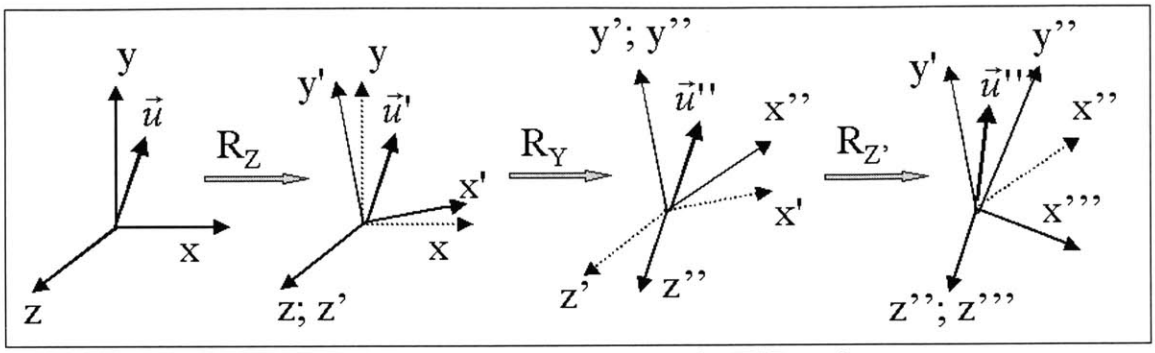


Figure A.4: Transformation sequence for ZYZ rotation

The equations below give a symbolic representation of the above figure.

$$\vec{u}' = R_Z \cdot \vec{u} \tag{A.9}$$
$$\vec{u}'' = R_Y \cdot \vec{u}' = R_Y \cdot R_Z \cdot \vec{u}$$
$$\vec{u}''' = R_{Z'} \cdot \vec{u}'' = R_{Z'} \cdot R_Y \cdot \vec{u}' = R_{Z'} \cdot R_Y \cdot R_Z \cdot \vec{u}$$

where $R_{z'yz}$ can be calculated using equation A.4 to A.8:

$$R_{ZYZ} = R_{Z\,Prime} \cdot R_Y \cdot R_Z =$$

$$= \begin{bmatrix} Cos[t] & Sin[t] & 0 \\ -Sin[t] & Cos[t] & 0 \\ 0 & 0 & 1 \end{bmatrix} \cdot \begin{bmatrix} Cos[a] & 0 & -Sin[a] \\ 0 & 1 & 0 \\ Sin[a]0 & 0 & Cos[a] \end{bmatrix} \cdot \begin{bmatrix} Cos[o] & Sin[o] & 0 \\ -Sin[o] & Cos[o] & 0 \\ 0 & 0 & 1 \end{bmatrix} =$$

$$= \begin{bmatrix} Cos[t] & Sin[t] & 0 \\ -Sin[t] & Cos[t] & 0 \\ 0 & 0 & 1 \end{bmatrix} \cdot \begin{bmatrix} Cos[a] \cdot Cos[o] & Cos[a] \cdot Sin[o] & -Sin[a] \\ -Sin[o] & Cos[o] & 0 \\ Cos[o] \cdot Sin[a] & Sin[a] \cdot Sin[o] & Cos[a] \end{bmatrix} =$$

$$= \begin{bmatrix} Cos[a] \cdot Cos[o] \cdot Cos[t] - Sin[0] \cdot Sin[t] & Cos[a] \cdot Cos[t] \cdot Sin[o] + Cos[0] \cdot Sin[t] & -Cos[t] \cdot Sin[a] \\ -Cos[t] \cdot Sin[o] - Cos[a] \cdot Cos[0] \cdot Sin[t] & Cos[o] \cdot Cos[t] - Cos[a] \cdot Sin[0] \cdot Sin[t] & Sin[a] \cdot Sin[t] \\ Cos[o] \cdot Sin[a] & Sin[a] \cdot Sin[o] & Cos[a] \end{bmatrix}$$

The angles $o$, $a$, and $t$ represent the three successive rotation (orientation) angles that reflect the relative orientation of frame B relative to frame A. Often, we need to solve for these three angles. The process is very simple and involve solving three equations with

three unknowns ($o$, $a$ and $t$). One solution for these three rotation angles using the ZYZ sequence is presented here.

$$Tan[o] = \frac{R_{ZYZ}(3,2)}{R_{ZYZ}(3,1)} = \frac{Sin[a] \cdot Sin[o]}{Sin[a] \cdot Cos[o]} \tag{A.13}$$

$$Tan[t] = \frac{R_{ZYZ}(2,3)}{R_{ZYZ}(1,3)} = -\frac{Sin[a] \cdot Sin[t]}{Sin[a] \cdot Cos[t]} \tag{A.14}$$

$$Tan[a] = \frac{R_{ZYZ}(3,1)}{R_{ZYZ}(3,3)} = \frac{Sin[a] \cdot Cos[o]}{Cos[a]} \tag{A.15}$$

[5]

A similar process can be done to solve for the transformation matrix using a YZX sequence.

$$R_Z = \begin{bmatrix} Cos[o] & Sin[o] & 0 \\ -Sin[o] & Cos[o] & 0 \\ 0 & 0 & 1 \end{bmatrix} \tag{A.16}$$

$$R_Y = \begin{bmatrix} Cos[a] & 0 & -Sin[a] \\ 0 & 1 & 0 \\ Sin[a]0 & 0 & Cos[a] \end{bmatrix} \tag{A.17}$$

$$R_X = \begin{bmatrix} 1 & 0 & 0 \\ 0 & Cos[t] & Sin[t] \\ 0 & -Sin[t] & Cos[t] \end{bmatrix} \tag{A.18}$$

$$R_{YZX} = R_X \cdot R_Z \cdot R_Y =$$

$$= \begin{bmatrix} Cos[a] \cdot Cos[o] & Sin[a] & -Cos[o] \cdot Sin[a] \\ -Cos[a] \cdot Cos[t] \cdot Sin[o] + Sin[a] \cdot Sin[t] & Cos[o] \cdot Cos[t] & Cos[t] \cdot Sin[a] \cdot Sin[o] + Cos[a] \cdot Sin[t] \\ Cos[t] \cdot Sin[a] + Cos[a] \cdot Sin[o] \cdot Sin[t] & -Cos[o] \cdot Sin[t] & Cos[a] \cdot Cos[t] - Sin[a] \cdot Sin[o] \cdot Sin[t] \end{bmatrix}$$

---

[5] Cos[o] is already known.

# Appendix B

# ROBOT PC COMMUNICATION

Listed below are the communication programs for both the robot and the PC.

## B.1 AS Code for Sending Robot Location to PC

```
'get the current location of the robot
HERE a
'break the current location into six components: X, Y, Z, O, A, T
DECOMPOSE x[0]=a
$out=""
For i=0 to 5 STEP 1
        $out=$out+$ENCODE(/F8.2,x[I]+","
END
Err=0
'Send through port 2 (serial) the 6 characters
SEND 2: $out, err
```

## B.2 VB Code for Receiving Robot Location from PC

```
Sub getFromRobot()
        Dim C() As Byte
        Dim arrayLength As Long
        Dim loopnum As Integer
        Dim i As Integer
        Dim msg As String
        MSComm1.CommPort = 1
        MSComm1.Settings = "9600,N,8,1"
        MSComm1.InputLen = 0
        MSComm1.handshaking = 3 'comRTSXon/xoff
        MSComm1.InputMode = comInputModeBinary
        MSComm1.PortOpen = True
handshaking:
        'ENQ ASCII 05
        'ACK ASCII 06
```

```
        While (MSComm1.InBufferCount = 0)
                DoEvents
        Wend
        C = MSComm1.Input
        If (C(0) = &H5) Then
                C(0) = &H6
                MSComm1.Output = C
        Else
                GoTo handshaking
        End If
        While (MSComm1.InBufferCount = 0) 'we need to wait for an input
                DoEvents
        Wend
        'once input was received check for the begining for the data ASCII 02
        C = MSComm1.Input
        If (C(0) = &H2) Then
                arrayLength = UBound(C)
                loopnum = 0  'use loop num to avoid infinite loop
                 msg = ""
                'data starts after ASCII 02
                For i = 1 To UBound(C)
                        msg = msg & Chr(C(i)) & ""
                Next i
                Do While (C(UBound(C)) <> &H3) '
                        DoEvents
                        If (MSComm1.InBufferCount <> 0) Then
                                C = MSComm1.Input
                                For i = 0 To UBound(C)
                                        msg = msg & Chr(C(i)) & ""
                                Next i
                        End If
                Loop
                C(0) = &H6
                MSComm1.Output = C
                'I need to separate these to 6 components (integer)
                Open FileName7 For Output As #1
                Pstart = Split(msg, ",")
                For i = 0 To 5
                        Print Format(Pstart(i), "0.000") & Space$(3);
                        Print #1, Format(Pstart(i), "0.0000  ")
                Next i
                Print
        End If
        MSComm1.PortOpen = False
End Sub
```

## B.3 AS Code for Receiving Robot Location from PC

```
'Receive data from the PC
err=0
RECEIVE 2: $inp, err
'Break down into 6 components
```

```
For i=0 to 5 STEP 1
        $temp=$DECODE($inp, ",", 0)
        loc[i]=VAL($temp)
        $temp==$DECODE($inp, ",", 1)
END
Point a= TRANS(loc[0], loc[1], loc[2], loc[3], loc[4]; loc[5])
'move robot to the new point a
Do Move a
```

## B.4 VB Code for Sending Robot Location to C Controller

```
Sub sendToRobot(msg As String)
        'define variables
        Dim a() As Byte
        Dim b() As Byte
        Dim i As Integer
        'define and open communication port
        MSComm1.CommPort = 1
        MSComm1.Settings = "9600,N,8,1"
        MSComm1.InputLen = 0
        MSComm1.handshaking = 3 'comRTSXon/xoff
        MSComm1.PortOpen = True
handshaking:
        'send ASCII 05
        ReDim a(0) As Byte
        a(0) = &H5
        MSComm1.Output = a
        'wait until we get an input
        While (MSComm1.InBufferCount = 0)
                DoEvents
        Wend
        'did we get ASCII 06?
        a = MSComm1.Input
        If (a(0) = &H6) Then
                'compose an ASCII "byte" that includes: ASCII 02, text, ASCII 03
                For i = 0 To Len(msg)
                        If i = 0 Then
                                a(0) = &H2
                        Else
                                ReDim Preserve a(0 To i)
                                a(i) = Asc(Mid(msg, i, 1))
                        End If
                Next i
                ReDim Preserve a(0 To i + 1)
                a(Len(msg) + 1) = &H3
                'send out to robot
                MSComm1.Output = a
        End If
        'we now need to confirm that the robot got the data. At this point, if the
        'data was received the robot sends an ACK
        'wait until we get an iput
        While (MSComm1.InBufferCount = 0)
```

```
                DoEvents
        Wend
        b = MSComm1.Input
        If (b(0) = &H6) Then
                'we need to send ASCII 04 - EOT
                b(0) = &H4
                MSComm1.Output = b
        End If
        'close the communication port
        MSComm1.PortOpen = False
End Sub
```

# Appendix C

# JR3 DSP DATA LOCATION

The table below summarizes the JR3 DSP data locations that are used by the DSP to perform variety of tasks.

| | 0x00 | 0x01 | 0x02 | 0x03 | 0x04 | 0x05 | 0x06 | 0x07 |
|---|---|---|---|---|---|---|---|---|
| 0x00 | ch0time | ch0data | | | ch1time | ch1data | | |
| 0x08 | ch2time | ch2data | | | ch3time | ch3data | | |
| 0x38 | chEtime | chEdata | | | chFtime | chFdata | | |
| 0x40 | 'C ' | 'o ' | 'p ' | 'y ' | 'r ' | 'i ' | 'g ' | 'h ' |
| 0x48 | 't ' | ' ' | 'J ' | 'R ' | '3 ' | ', ' | ' ' | 'l ' |
| 0x50 | 'n ' | 'c ' | ' ' | '1 ' | '9 ' | '9 ' | '4 ' | 0 |
| 0x58 | | | | | | | | |
| 0x60 | shunt fx | shunt fy | shunt fz | shunt mx | shunt my | shunt mz | | |
| 0x68 | def fs fx | def fs fy | def fs fz | def fs mx | def fs my | def fs mz | | load env # |
| 0x70 | min fs fx | min fs fy | min fs fz | min fs mx | min fs my | min fs mz | | xForm # |
| 0x78 | max fs fx | max fs fy | max fs fz | max fs mx | max fs my | max fs mz | | peak addr |
| 0x80 | fs fx | fs fy | fs fz | fs mx | fs my | fs mz | fs v1 | fs v2 |
| 0x88 | ofs fx | ofs fy | ofs fz | ofs mx | ofs my | ofs mz | ofs # | vect axes |
| 0x90 | f0 fx | f0 fy | f0 fz | f0 mx | f0 my | f0 mz | f0 v1 | f0 v2 |
| 0x98 | f1 fx | f1 fy | f1 fz | f1 mx | f1 my | f1 mz | f1 v1 | f1 v2 |
| 0xa0 | f2 fx | f2 fy | f2 fz | f2 mx | f2 my | f2 mz | f2 v1 | f2 v2 |
| 0xa8 | f3 fx | f3 fy | f3 fz | f3 mx | f3 my | f3 mz | f3 v1 | f3 v2 |
| 0xb0 | f4 fx | f4 fy | f4 fz | f4 mx | f4 my | f4 mz | f4 v1 | f4 v2 |
| 0xb8 | f5 fx | f5 fy | f5 fz | f5 mx | f5 my | f5 mz | f5 v1 | f5 v2 |
| 0xc0 | f6 fx | f6 fy | f6 fz | f6 mx | f6 my | f6 mz | f6 v1 | f6 v2 |
| 0xc8 | rate fx | rate fy | rate fz | rate mx | rate my | rate mz | rate v1 | rate v2 |
| 0xd0 | min fx | min fy | min fz | min mx | min my | min mz | min v1 | min v2 |
| 0xd8 | max fx | max fy | max fz | max mx | max my | max mz | max v1 | max v2 |
| 0xe0 | near sat | sat | rate addr | rate div | rate count | comm 2 | comm 1 | comm 0 |
| 0xe8 | count 1 | count 2 | count 3 | count 4 | count 5 | count 6 | errors | count x |
| 0xf0 | warning | error | threshold | crc | rom ver # | ver no | ver day | ver year |
| 0xf8 | serial | model | cal day | cal year | units | bits | chans | thickness |

# Appendix D

# LOAD CELL TARE LOAD – VB CODE

This VB program was written to account for the load cell – assemble fixture weight during the entire range of motion of the robotic test system.

```
'weight of load cell in Knee CS
W(1) = 46.5        'Fx Newtons
W(2) = 0'Fy
W(3) = 0'Fz

init_Mom(4) = 0
init_Mom(5) = 1.9251
init_Mom(6) = 0

Robot_loc = Split(point_to_robot, ",")

'xg, yg, zg, og, ag, tg are being used here - change to radians
x = Robot_loc(0)
y = Robot_loc(1)
z = Robot_loc(2)
o = Robot_loc(3) * PI / 180
a = Robot_loc(4) * PI / 180
t = Robot_loc(5) * PI / 180

'transform from tool to system zyz local to global
'we need to change the sign of the sin(angle)
'the output of the robot is (-) clockwise rotation
Roat(1, 1) = Cos(a) * Cos(o) * Cos(t) - Sin(o) * Sin(t)
Roat(1, 2) = -Cos(t) * Sin(o) - Cos(a) * Cos(o) * Sin(t)
Roat(1, 3) = Cos(o) * Sin(a)
Roat(2, 1) = Cos(a) * Cos(t) * Sin(o) + Cos(o) * Sin(t)
Roat(2, 2) = Cos(o) * Cos(t) - Cos(a) * Sin(o) * Sin(t)
Roat(2, 3) = Sin(a) * Sin(o)
Roat(3, 1) = -Cos(t) * Sin(a)
Roat(3, 2) = Sin(a) * Sin(t)
Roat(3, 3) = Cos(a)

'initializing the array
```

```
For i = 1 To 6
        aveF_M(i) = 0
Next i
' aveF_M(i) array (1) to (6)
For i = 1 To 6
        For f = 3 To (maxSample - 2)  'maxSample =10
                aveF_M(i) = (aveF_M(i) + datArray(f, i - 1))
        Next f
        aveF_M(i) = aveF_M(i) / (maxSample - 4)
        If i = 1 Then
                aveF_M(i) = aveF_M(i) + W(i)
        End If
        If i = 5 Then
                aveF_M(i) = aveF_M(i) + init_Mom(i)
        End If
Next i

'in global CS
W(1) = 0
W(2) = 0
W(3) = -46.5

'Force calculations
'F_Mloadcell(i + 1) array (1) to (6)
For i = 1 To 3
        F_Mloadcell(i) = 0  'zero forces  1-->3
        F_Mloadcell(i + 3) = 0  'zero moments 4-->6
        F_Mweight(i) = 0
        For j = 1 To 3
                F_Mweight(i) = F_Mweight(i) + Roat(j, i) * W(j)  'Roat transpose to get global
                to local
        Next j
        F_Mloadcell(i) = aveF_M(i) - F_Mweight(i)
Next i

'load cell CS
com(1) = 0.023      'X - units: meters
com(2) = 0          'Y
com(3) = 0.0414   'Z

'moments calculations M4, M5, M6
'1. multiplication of R(j,i)*W
'2. cross product com with result from 1
comRW_product(4) = com(2) * F_Mweight(3) - com(3) * F_Mweight(2)
comRW_product(5) = com(3) * F_Mweight(1) - com(1) * F_Mweight(3)
comRW_product(6) = com(1) * F_Mweight(2) - com(2) * F_Mweight(1)

'3. MOMENTS: subtract new value from the measured value
For i = 4 To 6
        F_Mloadcell(i) = aveF_M(i) - comRW_product(i)
Next i
```

# Appendix E

# VB CODE: COORDINATE SYSTEM ESTABLISHMENT

This VB program was written to construct coordinate systems for the load cell and the knee using digitized points recorded by the digitizer.

```
Private Sub cmdDigitize_Click()
        Dim FileName, FileName2 As String
        'digitized 6 points to determine knee coordinate system
        Dim Ax, Ay, Az, Bx, By, Bz, Cx, Cy, Cz, Dx, Dy, Dz, Ex, Ey, Ez, Fx, Fy, Fz As Double
        Dim Ofx, Ofy, Ofz, Otx, Oty, Otz As Double  'center of CS for femur and tibia respectively
        Dim Rkd(3, 3) As Double
        'dimensions for JR3
        Dim U1x, U1y, U1z, U2x, U2y, U2z, U3x, U3y, U3z As Double          'digitized 3 points
        Dim Oux, Ouy, Ouz As Double
        Dim Rld(3, 3) As Double
        Dim Rld_norm As Double
        'dimensions for translation vector and rotation matrix
        Dim rkl_d(3) As                 'translation wrt to digitizer
        Dim Rkd_T(3, 3) As Double       'rotation matrix
        Dim Rkd_norm As Double
        Dim Rlk(3, 3) As Double         'rotation matrix
        Dim rkl_k(3) As Double          'translation wrt to knee
        Dim i, j As Integer             'helping counter variables
        'Dimensions for center of load cell
        Dim rc(3) As Double             'distance between end and centre of load cell
        Dim rk(3) As Double             'rk=Rlk_T*rl
        Dim ABunitVec(3) As Double
        Dim EFunitVec(3) As Double
        Dim delta As Double
        Dim CosAngle As Double
        Dim dotProduct As Double

        'open digitized data from the following file
```

```
FileName = path & "digitizedata.txt"
Open FileName For Input As #11

'FileName2 = path & "Orthobasis.txt"
'Open FileName2 For Output As #12

'read digitized file
Do While Not EOF(11)
        Input #11, Ax, Ay, Az, Bx, By, Bz, Cx, Cy, Cz, Dx, Dy, Dz, Ex, Ey, Ez, Fx, Fy, Fz
Loop

'calcularing the unit vector for E-F line
EFunitVec(1) = (Ex - Fx) / Sqr((Ex - Fx) ^ 2 + (Ey - Fy) ^ 2 + (Ez - Fz) ^ 2)
EFunitVec(2) = (Ey - Fy) / Sqr((Ex - Fx) ^ 2 + (Ey - Fy) ^ 2 + (Ez - Fz) ^ 2)
EFunitVec(3) = (Ez - Fz) / Sqr((Ex - Fx) ^ 2 + (Ey - Fy) ^ 2 + (Ez - Fz) ^ 2)
'calcularing the unit vector for A-B line
ABunitVec(1) = (Ax - Bx) / Sqr((Ax - Bx) ^ 2 + (Ay - By) ^ 2 + (Az - Bz) ^ 2)
ABunitVec(2) = (Ay - By) / Sqr((Ax - Bx) ^ 2 + (Ay - By) ^ 2 + (Az - Bz) ^ 2)
ABunitVec(3) = (Az - Bz) / Sqr((Ax - Bx) ^ 2 + (Ay - By) ^ 2 + (Az - Bz) ^ 2)
'dot product
dotProduct = 0
For i = 1 To 3
        dotProduct = dotProduct + ABunitVec(i) * EFunitVec(i)
Next i
'calculating center of rotation for the femur
Ofx = (Ax + Bx) / 2
Ofy = (Ay + By) / 2
Ofz = (Az + Bz) / 2
Print "The origin of the knee is:"
Print Ofx, Ofy, Ofz
'Print #12, "The origin of the knee (femur) is:"
'Print #12, Ofx, Ofy, Ofz

'calculating deltaA, and deltaB
delta = Sqr((Ax - Bx) ^ 2 + (Ay - By) ^ 2 + (Az - Bz) ^ 2) * CosAngle / 2
'A,B new after reflected onto the global y axis
Ax = Ofx + delta * EFunitVec(1)
Ay = Ofy + delta * EFunitVec(2)
Az = Ofz + delta * EFunitVec(3)
Bx = Ofx - delta * EFunitVec(1)
By = Ofy - delta * EFunitVec(2)
Bz = Ofz - delta * EFunitVec(3)

'calculating center of rotation for the tibia
Otx = Ofx + (Dx - Cx)
Oty = Ofy + (Dy - Cy)
Otz = Ofz + (Dz - Cz)

'calculating the orthonormal basis for femur
'assume femur and tibia CS coincide
'*****
'horizontal matrix
'*****
'x axis
```

```
Rkd(1, 1) = (Ofx - Otx) / Sqr((Ofx - Otx) ^ 2 + (Ofy - Oty) ^ 2 + (Ofz - Otz) ^ 2)
Rkd(1, 2) = (Ofy - Oty) / Sqr((Ofx - Otx) ^ 2 + (Ofy - Oty) ^ 2 + (Ofz - Otz) ^ 2)
Rkd(1, 3) = (Ofz - Otz) / Sqr((Ofx - Otx) ^ 2 + (Ofy - Oty) ^ 2 + (Ofz - Otz) ^ 2)
'y axis
Rkd(2, 1) = (Ax - Bx) / Sqr((Ax - Bx) ^ 2 + (Ay - By) ^ 2 + (Az - Bz) ^ 2)
Rkd(2, 2) = (Ay - By) / Sqr((Ax - Bx) ^ 2 + (Ay - By) ^ 2 + (Az - Bz) ^ 2)
Rkd(2, 3) = (Az - Bz) / Sqr((Ax - Bx) ^ 2 + (Ay - By) ^ 2 + (Az - Bz) ^ 2)
'z axis
Rkd(3, 1) = Rkd(1, 2) * Rkd(2, 3) - Rkd(2, 2) * Rkd(1, 3)
Rkd(3, 2) = Rkd(1, 3) * Rkd(2, 1) - Rkd(2, 3) * Rkd(1, 1)
Rkd(3, 3) = Rkd(1, 1) * Rkd(2, 2) - Rkd(1, 2) * Rkd(2, 1)
'normalized z
Rkd_norm = Sqr(Rkd(3, 1) ^ 2 + Rkd(3, 2) ^ 2 + Rkd(3, 3) ^ 2)
Rkd(3, 1) = Rkd(3, 1) / Rkd_norm
Rkd(3, 2) = Rkd(3, 2) / Rkd_norm
Rkd(3, 3) = Rkd(3, 3) / Rkd_norm

'y cross z = x to ensure all are orthonormal
Rkd(1, 1) = Rkd(2, 2) * Rkd(3, 3) - Rkd(3, 2) * Rkd(2, 3)
Rkd(1, 2) = Rkd(2, 3) * Rkd(3, 1) - Rkd(3, 3) * Rkd(2, 1)
Rkd(1, 3) = Rkd(2, 1) * Rkd(3, 2) - Rkd(2, 2) * Rkd(3, 1)

'digitize JR3 to get CS
'FileName3 = path & "JR3Data.txt"
Open FileName3 For Input As #13
'FileName4 = path & "JR3Orthobasis.txt"
'Open FileName4 For Output As #14

'read digitized file
Do While Not EOF(13)
        Input #13, U1x, U1y, U1z, U2x, U2y, U2z, U3x, U3y, U3z
Loop

'calculating center of rotation for JR3
Oux = (U1x + U3x) / 2
Ouy = (U1y + U3y) / 2
Ouz = (U1z + U3z) / 2

Print "The origin of the load cell is:"
Print Oux, Ouy, Ouz
'Print #14, "The origin of the load cell is:"
'Print #14, Oux, Ouy, Ouz

'calculating the orthonormal basis for JR3
'*****
'horizontal matrix
'*****
'x axis
Rld(1, 1) = (Oux - U2x) / Sqr((Oux - U2x) ^ 2 + (Ouy - U2y) ^ 2 + (Ouz - U2z) ^ 2)
Rld(1, 2) = (Ouy - U2y) / Sqr((Oux - U2x) ^ 2 + (Ouy - U2y) ^ 2 + (Ouz - U2z) ^ 2)
Rld(1, 3) = (Ouz - U2z) / Sqr((Oux - U2x) ^ 2 + (Ouy - U2y) ^ 2 + (Ouz - U2z) ^ 2)
'y axis
Rld(2, 1) = (U1x - U3x) / Sqr((U1x - U3x) ^ 2 + (U1y - U3y) ^ 2 + (U1z - U3z) ^ 2)
Rld(2, 2) = (U1y - U3y) / Sqr((U1x - U3x) ^ 2 + (U1y - U3y) ^ 2 + (U1z - U3z) ^ 2)
```

```
Rld(2, 3) = (U1z - U3z) / Sqr((U1x - U3x) ^ 2 + (U1y - U3y) ^ 2 + (U1z - U3z) ^ 2)
'z axis
Rld(3, 1) = Rld(1, 2) * Rld(2, 3) - Rld(2, 2) * Rld(1, 3)
Rld(3, 2) = Rld(1, 3) * Rld(2, 1) - Rld(2, 3) * Rld(1, 1)
Rld(3, 3) = Rld(1, 1) * Rld(2, 2) - Rld(1, 2) * Rld(2, 1)
'normalized z
Rld_norm = Sqr(Rld(3, 1) ^ 2 + Rld(3, 2) ^ 2 + Rld(3, 3) ^ 2)
Rld(3, 1) = Rld(3, 1) / Rld_norm
Rld(3, 2) = Rld(3, 2) / Rld_norm
Rld(3, 3) = Rld(3, 3) / Rld_norm
'y cross z = x to ensure all are orthonormal
Rld(1, 1) = Rld(2, 2) * Rld(3, 3) - Rld(3, 2) * Rld(2, 3)
Rld(1, 2) = Rld(2, 3) * Rld(3, 1) - Rld(3, 3) * Rld(2, 1)
Rld(1, 3) = Rld(2, 1) * Rld(3, 2) - Rld(2, 2) * Rld(3, 1)

'Translation vector calculation rkl_d(i) wrt digitizer
rkl_d(1) = Ofx - Oux
rkl_d(2) = Ofy - Ouy
rkl_d(3) = Ofz - Ouz

Print "Translation vecotr (rkl_d):"
Print rkl_d(1), rkl_d(2), rkl_d(3)

'Final file includes translation data rkl_k
'FileName5 = path & "translation.txt"
Open FileName5 For Output As #15
'Final file inculdes rotation matrix Rlk
'FileName6 = path & "rotation.txt"
Open FileName6 For Output As #16

'Rotation matrix calculation
'Rdl^(-1)*Rdk=Rlk
'Rdk -Rotation matrix digitizer/knee
'Rdl -Rotation matrix digitizer/load cell
'Rdl^(-1)=Rdl^(T)=eJR3(3,3)
'Rlk -Rotation matrix load cell/knee

Print "Rdk Transpose (digitizer/knee):"
For i = 1 To 3
        rkl_k(i) = 0
        For j = 1 To 3
                Rkd_T(i, j) = Rkd(j, i)
                Print Format(Rkd_T(i, j), "0.000") & Space$(2);
                rkl_k(i) = rkl_k(i) + Rkd(i, j) * rkl_d(j)
                Next j
        Print
Next i

Print "Translation vecotr (rkl_k):"
For i = 1 To 3
        Print Format(rkl_k(i), "0.000") & Space$(3);
Next i
Print
```

```
Rlk(1, 1) = Rld(1, 1) * Rkd_T(1, 1) + Rld(1, 2) * Rkd_T(2, 1) + Rld(1, 3) * Rkd_T(3, 1)
Rlk(2, 1) = Rld(2, 1) * Rkd_T(1, 1) + Rld(2, 2) * Rkd_T(2, 1) + Rld(2, 3) * Rkd_T(3, 1)
Rlk(3, 1) = Rld(3, 1) * Rkd_T(1, 1) + Rld(3, 2) * Rkd_T(2, 1) + Rld(3, 3) * Rkd_T(3, 1)
Rlk(1, 2) = Rld(1, 1) * Rkd_T(1, 2) + Rld(1, 2) * Rkd_T(2, 2) + Rld(1, 3) * Rkd_T(3, 2)
Rlk(2, 2) = Rld(2, 1) * Rkd_T(1, 2) + Rld(2, 2) * Rkd_T(2, 2) + Rld(2, 3) * Rkd_T(3, 2)
Rlk(3, 2) = Rld(3, 1) * Rkd_T(1, 2) + Rld(3, 2) * Rkd_T(2, 2) + Rld(3, 3) * Rkd_T(3, 2)
Rlk(1, 3) = Rld(1, 1) * Rkd_T(1, 3) + Rld(1, 2) * Rkd_T(2, 3) + Rld(1, 3) * Rkd_T(3, 3)
Rlk(2, 3) = Rld(2, 1) * Rkd_T(1, 3) + Rld(2, 2) * Rkd_T(2, 3) + Rld(2, 3) * Rkd_T(3, 3)
Rlk(3, 3) = Rld(3, 1) * Rkd_T(1, 3) + Rld(3, 2) * Rkd_T(2, 3) + Rld(3, 3) * Rkd_T(3, 3)

Print "Rlk (load cell/knee):"
For i = 1 To 3
        For j = 1 To 3
                Print Format(Rlk(i, j), "0.000") & Space$(2);
                Print #16, Format(Rlk(i, j), "0.00000") & Space$(2);
        Next j
        Print
        Print #16,
Next i

'translation to center of load cell
rc(1) = 0
rc(2) = 0
rc(3) = 24.45  'mm

rk(1) = Rlk(3, 1) * rc(3)
rk(2) = Rlk(3, 2) * rc(3)
rk(3) = Rlk(3, 3) * rc(3)

'rkl_k between knee and CENTER of load cell
rkl_k(1) = rkl_k(1) + rk(1)
rkl_k(2) = rkl_k(2) + rk(2)
rkl_k(3) = rkl_k(3) + rk(3)

Print "NEW Translation vecotr (rkl_k):"
For i = 1 To 3
        Print Format(rkl_k(i), "0.000") & Space$(3);
        Print #15, Format(rkl_k(i), "0.00000") & Space$(3);
Next i
Print

Close #11
'Close #12
Close #13
'Close #14
Close #15
Close #16
```

End Sub

# Appendix F

# BROYDEN'S METHOD

A given problem involving $x_i$ variables gives N functional relationship to be zero:

$$F_i(x_1, x_2, .., x_N) = 0 \quad \text{i} = 1,2,..., \text{N} \tag{F.1}$$

The entire vector of values $x_i$ and as function $F_i$ can be define as $\vec{F}$ and $\vec{x}$, respectively. Using Taylor series expansion and neglecting all second and higher order terms, equation F.1 can be written as:

$$F_i(\vec{x} + \delta\vec{x}) = F_i(\vec{x}) + \sum_{k=1}^{N} \frac{\partial F_i}{\partial x_k} \delta x_k \tag{F.2}$$

The Jacobian matrix J is the matrix of partial derivatives shown in equation F.2:

$$J_{ik} = \frac{\partial F_i}{\partial x_k} \tag{F.3}$$

To obtain a set of linear equations that moves simultaneously each function closer to zero, equation F.2 is set to zero and the correction $\delta\vec{x}$ is calculated:

$$\boldsymbol{J} \cdot \delta\vec{\boldsymbol{x}} = -\boldsymbol{F} \tag{F.4}$$

Using LU decomposition the corrections to the solution vector can be calculated:

$$\vec{x}_{new} = \vec{x}_{old} + \delta\vec{x} \tag{F.5}$$

The main problem with the above approximation is the availability of the Jacobian matrix. For the knee joint system, the Jacobian is not known and therefore, another approximation to the Jacobian for zero finding is necessary.

C. G. Broyden [77] introduced a method for the Jacobian approximation. In this method, the $i^{th}$ quasi-Newton step $\delta x_i$ is the solution of:

$$B_i \cdot \delta\vec{x} = -F_i \tag{F.6}$$

Where $B_i$ is the Jacobian approximation. The quasi-Newton condition satisfies:

$$B_{i+1} \cdot \delta\vec{x} = F_{i+1} - F \equiv \delta F_i \tag{F.7}$$

Broyden showed that $B_{i+1}$ can be calculated using the following equation:

$$B_{i+1} = B_i + \frac{(\delta F_i - B_i \cdot \delta x_i) \otimes \delta x_i}{\delta x_i \cdot \delta x_i} \tag{F.8}$$

Using the Sherman-Morrison formula, equation F.8 can be inverted analytically:

$$B_{i+1}^{-1} = B_i^{-1} + \frac{(\delta x_i - B_i^{-1} \cdot \delta F_i) \otimes \delta x_i \cdot B_i^{-1}}{\delta x_i \cdot B_i^{-1} \cdot \delta F_i} \tag{F.9}$$

The solution for $\delta x_i$ is now possible using:

$$\delta x_i = -B_i^{-1} \cdot F_i \tag{F.10}$$

# BIBLIOGRAPHY

[1] G. J. Smidt, "Biomechanical analysis of knee flexion and extension," *J. Biomech*, vol. 6, pp. 79-92, 1973.

[2] S. Hirokawa, "Biomechanics of the knee joint: A critical review," *Critical Rev Biomed Eng.*, vol. 21, pp. 79-135, 1993.

[3] M. Nordin and V. H. Frankel, "Biomechanics of the Knee," in *Biomechanics of Joints*, pp. 115-134.

[4] R. Cailliet, *Knee Pain and Disability*: F. A. Davis Company, 1974.

[5] T. Wright and S. Goodman, "What is the clinical scope of the wear-related problem?," in *Implant Wear: The Future of Total Joint Replacement*, T. Wright and S. oodman, Eds. Rosemont, IL: AAOS, 1996.

[6] J. Insall, "Presidential address to the knee society - Choices and compromises in total knee arthroplasty," *Clin Ortho*, vol. 226, pp. 43-48, 1988.

[7] J. R. Moreland, "Mechanisms of Failure in Total Knee Arthroplasty," *Clinical Orthopedics and Related research*, vol. No. 226, pp. 49-64, 1988.

[8] T. Andriacchi and J. Galante, "Retention of the posterior cruciate in total knee arhtroplasty," *J Arthroplasty*, vol. Supplement, pp. S13-S19, 1988.

[9] W. Lew and J. Lewis, "The effect of knee-prosthesis geometry on cruciate ligament mechanics during flexion," *JBJA*, vol. 64-A, pp. 734-739, 1982.

[10] S. Stern and J. Insall, "Posterior stabilized prosthesis: results after follow-up of nine to twelve years," *J Bone Joint Surg*, vol. 74A, pp. 980-986, 1992.

[11] R. Singerman, J. Dean, H. Pagan, and V. Goldberg, "Decreased posterior tibial slope increases strain in the posterior cruciate ligament following total knee arthroplasty," *J Arthroplasty*, vol. 11, pp. 99-103, 1996.

[12] J. Arima, L. Whiteside, J. Martin, H. Miura, S. White, and D. McCarthy, "Effect of partial release of the posterior cruciate ligament in total knee arthroplasty," *Clin Ortho*, vol. 353, pp. 194-202, 1998.

[13] D. Dennis, R. Komistek, W. Hoff, and S. Gabriel, "In-vivo knee kinematics derived using an inverse perspective technique," *Clin Ortho*, vol. 331, pp. 107-117, 1996.

[14] S. Incavo, C. Johnson, B. Beynnon, and J. Howe, "Posterior cruciate ligament strain biomechanics in total knee arthroplasty," *Clin Ortho*, vol. 309, pp. 88-93, 1994.

[15] O. Mahoney, P. Noble, D. Rhoads, J. Alexander, and H. Tullos, "Posterior cruciate function following total knee arthroplasty," *J Arhtoplasty*, vol. 9, pp. 569-578, 1994.

[16] J. Andrews and A. MJ, "The classification of knee ligament instability," *Orthop Clin North Am*, vol. 16, pp. 69-82, 1985.

[17] L. Detenbeck, "Function of the cruciate ligaments in knee stability," *Am J Sports Med*, vol. 2, pp. 217-221, 1974.

[18] J. C. Hughston, J. R. Andrews, M. J. Cross, and A. Moschi, "Classification of knee ligament instabilities Part I. The medial compartment and cruciate ligaments," *Journal of Bone and Joint Surgery*, vol. 58-A, pp. 159-72, 1976.

[19] J. C. Hughston, J. R. Andrews, M. J. Cross, and A. Moschi, "Classification of knee ligament instabilities Part II. The lateral compartment," *Journal of Bone and Joint Surgery*, vol. 58-A, pp. 173- 9, 1976.

[20] G. Bessette and R. Hunter, "The anterior cruciate ligament," *Orthopedics*, vol. 13, pp. 551-562, 1990.

[21] J. R. Seebacher, A. E. Inglis, J. L. Marshall, and R. F. Warren, "The structure of the posterolateral aspect of the knee.," *Journal of Bone and Joint Surgery*, vol. 64A, pp. 536-541, 1982.

[22] V. C. Mow and W. C. Hayes, *Basic Orthopedic Biomechanics*, 1991.

[23] J. P. Fulkerson and D. S. Hungerford, *Disorder of the patellofemoral joint*, 2nd Edition ed, 1977.

[24] L. Blankevoort and R. Huiskes, "Ligament-bone interaction in a three-dimensional model of the knee," *J. Biomech. Eng.*, vol. 113, pp. 263-269, 1991.

[25] L. Blankevoort and R. Huiskes, "ACL isometry is not the criterion for ACL reconstruction," *Trans ORS*, vol. 16, pp. 203, 1991.

[26] E. Abdel-Rahman and M. S. Hefzy, "A two-dimensional dynamic anatomical model of the human knee joint," *J. Biomech. Eng.*, vol. 115, pp. 357-365, 1993.

[27] E. H. Chen and J. Black, "Materials design analysis of the prosthetic anterior cruciate ligament," *Journal of Biomedical Materials Research*, vol. 14, pp. 567-586, 1980.

[28] J. M. Hollis, "Development and application of a method for determining the in-situ forces in anterior cruciate ligament bundles," : University of California, San Diego (UCSD), 1988.

[29] J. L. Lewis, W. D. Lew, P. Hanley, S. Kirstukas, R. Hunter, and C. Kowalczyk, "Variability and load sharing in ACL repairs," *Trans ORS*, vol. 13, pp. 127, 1988.

[30] J. L. Lewis, W. D. Lew, and J. Schmidt, "Description and error evaluation of an in-vitro knee joint testing system," *J. Biomech. Eng.*, vol. 110, pp. 238-248, 1988.

[31] G. S. Berns, M. L. Hull, and H. A. Patterson, "Implementation of a five degree of freedom automated system to determine knee flexibility in vitro," *J. Biomech. Eng.*, vol. 112, pp. 392-400, 1990.

[32] M. J. Hollis, "Use of a six degree of freedom position control actuator to study joint kinematics," *ASME Adv. in Bioeng.*, vol. BED-20, pp. 409-411, 1991.

[33] S. Takai, G. A. Livesay, S. L.-Y. Woo, D. J. Adams, and F. H. Fu, "Determination of the in-situ loads on the human anterior cruciate ligament," *J. Orthop. Res.*, vol. 11, pp. 686-695, 1993.

[34] M. A. Lafortune, P. R. Cavanagh, H. J. Sommer, and A. Kalenak, "Three-dimensional kinematics of the human knee during walking," *J. Biomech*, vol. 25, pp. 347-357, 1992.

[35] C. Reinschmidt, A. J. van den Bogert, B. M. Nigg, A. Lundberg, and N. Murphy, "Effect of skin movement on the analysis of skeletal knee joint motion during running," *J. Biomech*, vol. 30, pp. 729-732, 1997.

[36] J. D. Reuben, J. S. Rovick, P. S. Walker, and R. J. Schrager, "Three-dimensional kinematics of normal and cruciate deficient knees - A dynamic in-vitro experiment," *Trans ORS*, vol. 11, pp. 385, 1986.

[37] J. D. Reuben, J. S. Rovick, R. J. Schrager, P. S. Walker, and A. L. Boland, "Three-dimensional dynamic motion analysis of the anterior cruciate ligament deficient knee joint," *Am. J. Sports Med.*, vol. 17, pp. 463-471, 1989.

[38] P. S. Trent, P. S. Walker, and P. Wolf, "Ligament length patterns, strength and rotational axes of the knee joint," *Clin. Orthop. Rel. Res.*, vol. 117, pp. 263-270, 1976.

[39] S. J. Kirstukas, J. L. Lewis, and A. G. Erdman, "6R instrumented spatial linkages for anatomical joint motion measurement - Part 1: Design," *J. Biomech. Eng.*, vol. 114, pp. 92-100, 1992.

[40] H. Kurosawa, P. S. walker, S. Abe, A. Garg, and T. Hunter, "Geometry and Motion of he Knee for Implant and Orthotic Design," *Journal of Biomechanics*, vol. 18, pp. 487-499, 1985.

[41] S. R. Simon, H. W. Trieschmann, R. G. Burdett, F. C. Ewlad, and C. B. Sledge, "Quantitative gait analysis after total knee arthroplasty for monarticular degenerative asthritis," *JBJS*, vol. 65-A, pp. 605, 1983.

[42] K. L. Markolf, J. S. Mensch, and H. C. Amstutz, "Stiffness and laxity of the knee - the contributions of the supporting structures," *Journal of Bone and Joint Surgery*, vol. 58A, pp. 583-593, 1976.

[43] S. Nielsen, J. Ovesen, and R. O., "The anterior Cruciate ligament of the Knee," *Arch Orthop Trauma Surg*, vol. 104, pp. 357-362, 1984.

[44] H.-H. Hsieh and P. S. Walker, "Stabilizing Mechanisms of the Loaded and Unloaded Knee Joint.," *Journal of Bone and Joint Surgery*, vol. 58-A, pp. 87-93, 1976.

[45] R. L. Piziali, W. P. Seering, D. A. Nagel, and D. J. Schurman, "The function of the primary ligaments of the knee in anterior-posterior and medial-lateral motions," *J. Biomech*, vol. 13, pp. 777-784, 1980.

[46] R. L. Piziali, J. Rastager, D. A. Nagel, and D. J. Schurman, "The contributions of the cruciate ligaments to the load-displacement characterisitics of the human knee joint," *J. Biomech. Eng.*, vol. 102, pp. 277-283, 1980.

[47] K. Markolf, W. Bargar, S. Shoemaker, and H. Amstutz, "The role of joint load in knee stability," *Journal of Bone and Joint Surgery*, vol. 63A, pp. 570-585, 1981.

[48] E. Y. S. Chao, "Justification of a triaxial goniometer for the measurement of joint rotation," *J. Biomech*, vol. 13, pp. 989-1006, 1980.

[49] P. S. Walker and J. V. Hajek, "The load-bearing area in the knee joint," *J. Biomech*, vol. 5, pp. 581-589, 1972.

[50] L. Blankevoort and R. Huiskes, "An alternative rotation restraint in the knee joint," *Trans ORS*, vol. 14, pp. 26, 1989.

[51] L. Blankevoort, R. Huiskes, and A. de Lange, "Helical axes along the envelope of passive knee joint motion," *Trans ORS*, vol. 11, pp. 410, 1986.

[52] L. Blankevoort, R. Huiskes, and A. de Lange, "The envelope of passive knee joint motion," *J. Biomech*, vol. 21, pp. 705-720, 1988.

[53] L. Blankevoort, R. Huiskes, and A. de Lange, "Helical axes of passive knee joint motions," *J. Biomech*, vol. 23, pp. 1219-1229, 1990.

[54] R. v. Dijk, R. Huiskes, and G. Selvick, "Roentgen stereophotogrammetric methods for the evaluation of the three dimensional kinematic behaviour and cruciate ligament length patterns of the human knee joint," *J. Biomech*, vol. 12, pp. 727-731, 1979.

[55] J. Karrholm, L.-G. Elmqvist, G. Selvik, and L. I. Hansson, "Chronic anterolateral instability of the knee: A roentgen stereophotogrammetric evaluation," *Am. J. Sports Med.*, vol. 17, pp. 555-563, 1989.

[56] A. d. Lange, R. Huiskes, and J. M. G. Kauer, "Measurement errors in roentgen-stereophotogrammetric joint-motion analysis," *J. Biomech*, vol. 23, pp. 259-269, 1990.

[57] R. Huiskes, J. Kremers, A. de Lange, H. J. Woltring, G. Selvik, and T. J. G. van Rens, "Analytical stereophotogrammetric determination of three-dimensional knee-joint geometry," *J. Biomech*, vol. 18, pp. 559-570, 1985.

[58] E. S. Grood, W. J. Suntay, F. R. Noyes, and D. L. Butler, "Biomechanics of the knee-extension exercise," *J. Bone Joint Surg.*, vol. 66A, pp. 725-734, 1984.

[59] G. L. Kinzel, A. S. Hall Jr, and B. M. Hillberry, "Measurement of the total motion between two body segments - I. Analytical development," *J. Biomech*, vol. 5, pp. 93-105, 1972.

[60] G. L. Kinzel, B. M. Hillberry, A. S. Hall Jr, D. C. Van Sickle, and W. M. Harvey, "Measurement of the total motion between two body segments - II. Description of application," *J. Biomech*, vol. 5, pp. 283-293, 1972.

[61] H. Fujie, K. Mabuchi, S. L.-Y. Woo, G. A. Livesay, S. Arai, and Y. Tsukamoto, "The use of robotics technology to study human joint kinematics: A new methodology," *J. Biomech. Eng.*, vol. 115, pp. 211-217, 1993.

[62] T. Rudy, G. A. Livesay, J. W. Xerogeanes, Y. Takeda, F. H. Fu, and S. L.-Y. Woo, "A combined robotics/UFS approach to measure knee kinematics and determine in-situ ACL forces," *ASME Advances in Bioengineering*, vol. BED-28, pp. 287-288, 1994.

[63] H. Fujie, K. Mabuchi, Y. Tsukamoto, M. Yamamoto, and T. Sasada, "A new method of human knee diagnosis using robotics," presented at First World Congress of Biomechanics, La Jolla, CA, 1990.

[64] H. Fujie, G. A. Livesay, K. Mabuchi, Y. Tsukamoto, and S. L.-Y. Woo, "A new methodology to perform joint kinematics studies using robotics," *ASME Advances in Bioengineering*, vol. BED-20, pp. 407-408, 1991.

[65] H. Hirsch, P. Lotke, and L. Morrison, "The posterior cruciate ligament in total knee aurgery," *Clin Ortho*, vol. 309, pp. 64-68, 1994.

[66] T. Andriacchi and J. Galante, "Influences of total knee replacement design on walking and climbing," *J Bone Joint Surg*, vol. 64A, pp. 1328-1335, 1982.

[67] P. Lewandowski, M. Askew, D. Lin, F. Hurst, and A. Melby, "Kinematics of posterior cruciate ligament-retaining and -sacrificing mobile bearing total knee arthroplasty," *J Arthroplasty*, vol. 12, pp. 777-784, 1997.

[68] R. Worland, D. Jessup, and J. Johnson, "Posterior cruciate recession in total knee arthroplasty," *J Arthroplasty*, vol. 12, pp. 70-73, 1997.

[69] M. Freeman and G. Railton, "Should the posterior cruciate ligament be retained or resected in condylar nonmeniscal knee arthroplasty," *J Arthroplasty*, vol. Supplement, pp. S3-S12, 1988.

[70] J. Stiehl, R. Komistek, D. Dennis, and R. Paxson, "Fluoroscopic analysis of kinematics after posterior-cruciate-retaining knee arthroplasty," *J Bone Joint Surg*, vol. 77-B, pp. 884-889, 1995.

[71] H. Kim, R. Pelker, D. Gibson, J. Irving, and J. Lynch, "Rollback in posterior cruciate ligament-retaining total knee arthroplasty," *J Arthroplasty*, vol. 12, pp. 553-561, 1997.

[72] M. Ritter, S. Herbst, E. Keating, P. Paris, and J. Meding, "Long-term survival analysis of a posterior cruciate-retaining total condylar total knee arthroplasty," *Clin Ortho*, vol. 309, pp. 136-145, 1994.

[73] D. Pereira, F. Jaffe, and C. Ortiguera, "Posterior cruciate ligament0sparing versus posterior cruciate ligament sacrificing arthroplasty," *J Arthroplasty*, vol. 13, pp. 138-144, 1998.

[74] R. Laskin and H. O'Flynn, "Total knee replacement with posterior cruciate ligament retention in rheumatoid arthritis," *Clin Ortho*, vol. 345, pp. 24-28, 1997.

[75] P. Lattanzio, D. Chess, and J. MacDermid, "Effect of the posterior cruciate ligament in knee-joint proprioception in total knee arthroplasty," *J Arthroplasty*, vol. 13, pp. 580-585, 1998.

[76] G. Li, T. W. Rudy, M. Sakane, A. Kanamori, C. B. Ma, and S. L. Y. Woo, "The importance of quadriceps and hamstrings muscle loading on knee kinematics and in-situ forces in the ACL," *J Biomechanics*, vol. 32, pp. 395-400, 1999.

[77] C. G. Broyden, *Mathematics of Computation*, vol. 19, 1965.

[78] Ellis R and G. D, *Calculus with analytic geometry*, 1990.

[79] G. Li, T. W. Rudy, C. Allen, M. Sakane, and S. L. Y. Woo, "Effect of combined axial compressive and anterior tibial loads on in-situ forces in the anterior tibial ligament: A porcine study," *J. Orthop. Res.*, vol. 16, pp. 122-127, 1998.

[80] T. W. Rudy, G. A. Livesay, S. L.-Y. Woo, and F. H. Fu, "A combined robotics/universal force sensor approach to determine in-situ forces of knee ligaments," *J. Biomech*, vol. 29, pp. 1357-1360, 1996.

[81] W. H. Press, S. A. Teukolsky, W. T. Vetterling, and B. P. Flannery, *Numerical Recipes*. New York: Cambridge University Press, 1992.

[82] G. Strang, *Linear Algebra and Its Applications*, 2nh ed, 1980.

[83] Cheng H and K. K. C., "An historical note on finite rotations," *J. Applied Mechanics*, vol. 56, pp. 139-145, 1989.

[84] http://www.hughston.com/hha/a.11.2.1.htm.

[85] http://www.hughston.com/hha/a.extmech.htm.